

We are IntechOpen, the world's leading publisher of Open Access books Built by scientists, for scientists

6,900

Open access books available

186,000

International authors and editors

200M

Downloads

Our authors are among the

154

Countries delivered to

TOP 1%

most cited scientists

12.2%

Contributors from top 500 universities



WEB OF SCIENCE™

Selection of our books indexed in the Book Citation Index
in Web of Science™ Core Collection (BKCI)

Interested in publishing with us?
Contact book.department@intechopen.com

Numbers displayed above are based on latest data collected.
For more information visit www.intechopen.com



Nanocomposite Based Multifunctional Coatings

Horst Hintze-Bruening and Fabrice Leroux

Additional information is available at the end of the chapter

<http://dx.doi.org/10.5772/46853>

1. Introduction

The function of automotive coatings so far has been twofold – decoration and conservation. The former not only consists of providing a coloured and smooth surface but also to accentuate the shape of the car body via a viewing angle dependant brightness and / or colour. These optical effects mostly rely on tiny mirrors of metal flakes like aluminium or coated mica platelets that are more or less homogeneously dispersed within one coating layer; their surface normal predominantly being orthogonal to the substrates surface. The particles lateral dimensions typically are in the order of several hundred microns. The role of the coatings in the conservation of a metallic car body mainly consists in the protection of the substrate towards electrochemical degradation (= corrosion) either actively or via providing a barrier layer as well as a best possible limitation of the coatings defects produced in the wake of dramatic mechanical perturbations like impacting gravel stones. On the contrary mounted plastic parts or body panels in most cases have to be protected against chemical degradation triggered by exposure to UV light, physical erosion by swelling solvents like fuel or water depending on the nature of the polymers and the morphology of the bulk as well as towards catastrophic failure of the part upon mechanical impacts (= brittle crash behaviour). The means to achieve the latter are similar to those that are used in the design of stone chip resistant coatings for car bodies.

The present chapter describes the potential use of nano scaled particles based polymer composites as multifunctional constituents for novel protective as well as decorative automotive coatings. The focus lies on composites based on layered particles, namely layered double hydroxides (= LDH), their beneficial mechanical modes of action for energy dissipation, their diffusion barrier properties as well as their role in the active corrosion inhibition. For other coatings related applications of these materials we refer to a separate review article (Leroux et al., 2012).

2. Background

2.1. Automotive coatings

Since the industrialization of the car manufacturing process today's automotive coatings have been optimized in an evolutionary process over the past decades resulting in a typical stack of highly specialized individual coating layers (Fig. 1). This comprises an initially cathodic electrodeposited material that provides adhesion and active corrosion inhibition (ED coat) which then is covered by a spray coated layer (= primer) for the smoothening and protection of the ED coat towards UV light. On to the primer surface two layers are consecutively spray applied: first a "base coat" that provides the colour followed by a transparent top coat (= clear coat) which renders the whole system bright, smooth as well as resistant towards chemicals (bird droppings, tar, rosin, acid rain) and surface related mechanical impact like the scratching in the course of car washing. Except for the base coat itself all other layers are chemically cured after physical drying and film formation which implies that the car body has to pass three bake cycles up to 170°C (ED) or 140°C (combined base and clear layer).

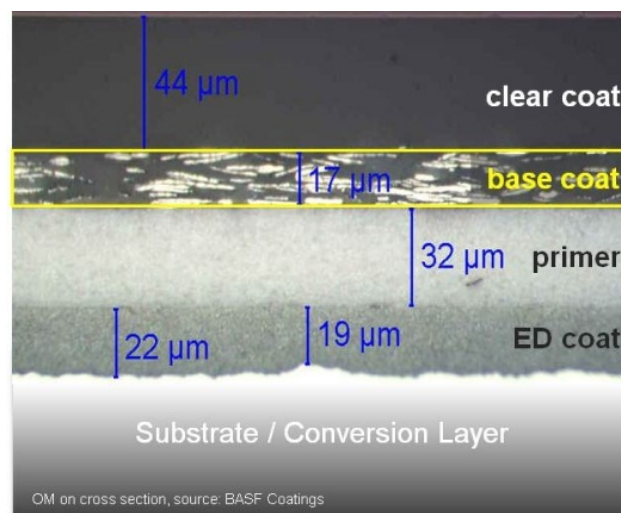


Figure 1. Automotive coating system applied on pretreated metal.

In order to render this coating process more eco-efficient some novel coating systems recently have been introduced which comprise stacks with a reduced number of layers, e.g. without the primer (Fig. 2), (Kreis, 2008). Under critical conditions such lean coatings reveal an insufficient capability to maintain the high level of performance of their technically more mature predecessors.

This is the setting for the development of new material concepts that may provide solutions capable to overcome the constraints inherent to these recent coatings systems which are still essentially based on the conventional technologies. With respect to the automotive coatings conservation functionality it has to be pointed out that – contrary to that what is sometimes suggested by textbooks and patent claims – some features are not attributed exclusively to one single layer, e.g. the relation of the primer layers properties and the stone chip

resistance of the coating. Thus, although typically tested and introduced within one coating layer, the potential use of the described new materials concepts should not be considered to be restricted to these prototypes, substrates and applications respectively.

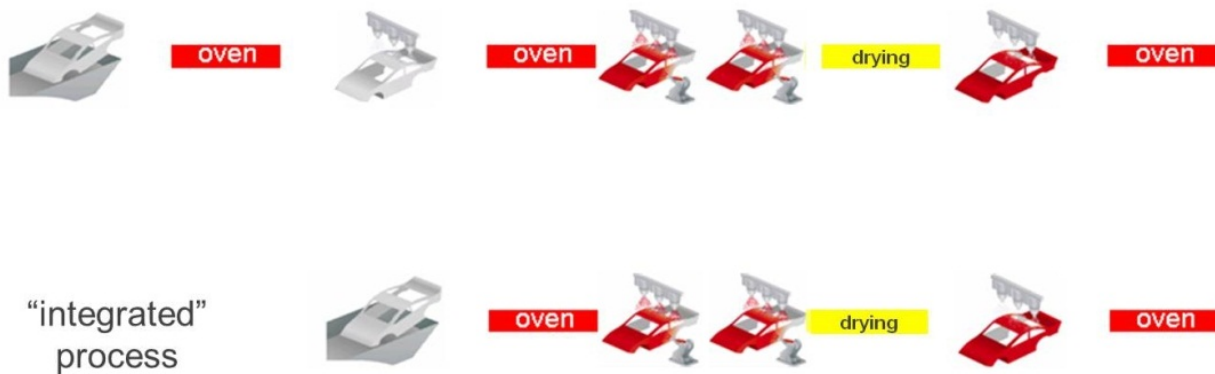


Figure 2. Conventional automotive coating process compared to novel integrated coating.

2.2. Stone impact

Gravel stone impingement is an occasional though dramatic event in the lifetime of an automotive body or mounted part and has intensively been studied (Zehnder et al., 1993; Ramamurthy et al., 1994; Zouari & Touratier, 2002; Lonyuk et al., 2007).

Regarding the physical processes occurring in a coating system there are three common basic features aside from all conceivable differences in terms of inclination angle, kinetic energy (up to 100 m/s, mass of projectiles up to several grams) as well as the shape (curvature radius) of the projectile:

1. Short time scales (micro seconds) and a very limited impact area smaller than one mm² are the features of an adiabatic process which yields a local heating (up to 10²K) and a propagating shock wave.
2. A central compression area where the substrate plastically might deform and the coating material gets crunched is surrounded by a strained zone due to the lateral displacement of the coating material by the impinging projectile – thus shear stress in a transition zone causes coatings delamination.
3. The volume of laterally displaced coating material reaches its maximum towards the coatings surface – thus within the highly cross linked top coat which can least accommodate by plastic flow. Hence compressive and tensile stresses (depending on the inclination angle and shape of the object) yield crack initiation within this layer and crack propagation throughout the entire coating system.

This simplified scenario varies with different impact events as evidenced by comparing an orthogonal crush of a blunt object (infinite curvature radius) with the orthogonal “denting” of spiky or edged gravel or with the inclined “carving” by an edged impinging projectile (Dhar et al., 2005). Figure 3a shows the crater produced by a single spherical impact. Radial and concentric cracks as well as plastically flown coatings material encircle a central spot of

crunched coating. The plastically deformed metal substrate and the coatings delamination at the interface with the conversion layer (bonder) is displayed after the removal of the damaged coating material using an adhesive tape (Figure 3b). In real life gravel stones are irregularly formed and they may impact under all conceivable inclination angles. Thus all coatings damage symptoms between "denting" and "carving" are summarized as "stone chipping".

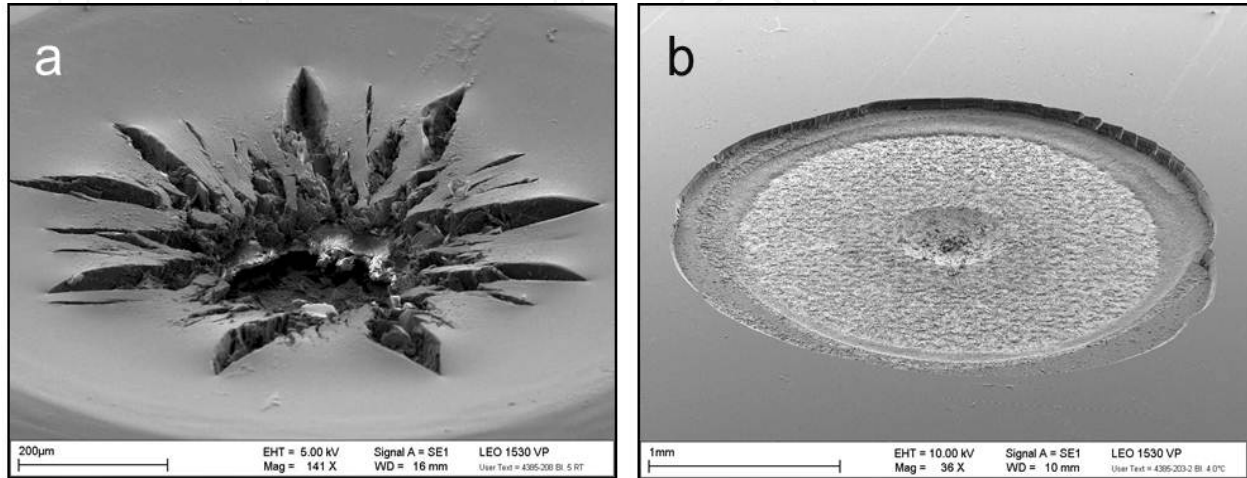


Figure 3. Impact crater on a coated test panel after an orthogonal single spherical impact (steel, 0,03g, $d=2\text{mm}$, $v=70\text{ m/s}$, $T=273\text{K}$) before (a) and after (b) removal of damaged coating. Scale bars are $200\mu\text{m}$ (a) and 1mm (b).

Standardized test methods have been established to assess the resistance of a coated work-piece against stone chipping. They consist of multiple impacts of accelerated gravels or steel grit particles on a defined area of a coated panel and a subsequent visual rating of the damage as well as a standardized image data processing of the exposed area. This latter procedure allows for the assessment of the area percentages of the uncovered substrate as well as the interfacial and cohesive fracture planes within the coating itself, provided appropriate thresholds can be defined to differentiate between these fracture sites. For the allocation of the uncovered metal surface the panel is immersed into a copper salt solution in order to get deposited elemental copper. Some tests specify that the impacted panels are exposed to aggressive environments in order to provoke the corrosion of the substrate which predominantly sets in at those damaged spots that bear bare metal surface.

The ratio of flow and cracking as well as the extent of the delamination zone depend on the film thickness and of the materials properties like the glass transition temperature (Lonyuk et al., 2008), the crosslink density (Bender, 1969), the interlayer adhesive strength (Ryntz et al., 1995) and finally the coatings morphology.

The importance of the latter has recently been highlighted with respect to the "conflicts between strength and toughness" in terms of the intrinsic fracture mechanics operating ahead the tip of a promoting crack (Ritchie, 2011). Making reference to hierarchical materials the author outlines the possibility to "attain both properties in a single material through the presence of multiple plasticity and toughening mechanisms acting on different length-

scales". Within section 3.2. of this chapter we describe possibilities to translate these design principles into stone impact resistant coating materials that are based on multiple scale heterogeneity.

2.3. Automotive primer

Besides the smoothening and the protection of the ED coating layer against UV light the stone chip resistance of an automotive coating system is often attributed to the primer layer. Although the failure mode of any multilayer coating upon such a mechanical impact also depends on the characteristics of all individual layers (Dioh & Williams, 1994; Rutherford et al., 1997) the typical composition as well as the morphology of an automotive primer layer are somehow appropriate to mitigate the action of propagating cracks as well as the dislocation and crushing of the material.

In the first instance the organic fraction typically consists of weakly cross linked rather high molecular weight polymers that are bearing sites for hydrogen bonding. By a proper choice of the polyisocyanates as well as the polyols and / or the polyamines – the complementary reactants that yield polyurethanes or polyureas respectively via a step growth poly addition reaction – bulk materials can be obtained that segregate into rigid domains bearing hydrogen bonds between adjacent urethane / urea building blocks and soft domains linking the former. These soft segments typically consist of polyether diols or polyester diols that possess a high segment flexibility – which manifests in a low glass transition temperature (T_g). This flexibility in combination with the reversible breaking and formation of hydrogen bonds provides a pronounced toughness to the polymer phase. These polymers usually comprise rather low functionalities for chemical cross linking like hydroxyl groups. Typical values for "hydroxyl numbers"¹ are below 50 distributed over largely uneven chain lengths with mean molecular weights (M_n) in the order of 10^4 to 10^6 and typical polydispersity indices² (M_w/M_n) between 3 and 4. Therefore it is common to use them in admixture with more resinous hydroxyl functional polymers like polyesters and / or in combination with crosslinking agents like alkoxylated melamine formaldehyde resins. Under acid catalysis and with increasing temperature the latter either react with the hydroxyl groups of the former or they self-polymerize via transesterification. Depending on the overall formulation and the presence of internal interfaces due the presence of e.g. pigment particles the self-condensation of the MF resin may yield an additional heterogeneity of the polymer phase due to a pronounced anisotropic alignment of the aromatic melamine cores. This was also found to form hierarchical ordered structures over several length scales in the heterophasic self-condensation of hexamethoxy melamine formaldehyde resin in water (Weber et al., 2009). Besides the intrinsic toughness of the polymer phase stemming from the main chain segment flexibility and the intermolecular formation of reversible hydrogen bonds which favour plastic

¹ Hydroxyl- as well as acid numbers are defined as the amount of potassium hydroxide that would be consumed for the neutralization of these Brønstedt acids present within one gram of the solid (= nonvolatile) material. They are given as "mg KOH/g".

² Mean mass molecular weight (M_w) and mean number molecular weight (M_n) of polymers to be obtained from e.g. size exclusion chromatography.

deformation the heterogenization of the polymer phase due to segregation and polymer incompatibility might impede both crack initiation and propagation. This is well known from the impact behaviour of plastic parts where a more rigid mostly continuous phase imparts a soft second polymer phase as an impact modifier and the particular morphology of bicontinuous polymer phases was proposed as beneficial for stone impact resistant automotive primer layers (Makowski et al., 2005). The softer phase is attributed to release stress at the tip of cracks by stress reallocation and dissemination. Thus the softest conceivable material would be an included gaseous phase as nearly everyone's mundane experience with polymer foams or materials scientists work in the field of tough porous ceramics expressively attest (Studart et al., 2006). Indeed breakable hollow spheres have been proposed as impact modifying loci for stone chip resistant coatings (Roesler et al., 1997).

However these polymer matrices normally are filled with rather high amounts of inorganic pigments like titania (TiO_2), barite (BaSO_4) and fillers like precipitated calcium carbonate (CaCO_3) and talc (layered silicate minerals) – the particle sizes of the latter being in the micrometre range. In the course of a stone impact event such a composite mechanically dissipates energy via the damping of a traversing shock wave where the conservation of momentum commensurate to the mass, acts as a ballast bed via interlocking coarse particles thus disseminating stress or it fails at predetermined breaking points respectively. This latter manifests in the fracture surface of primer layers that comprise such clay minerals like talc or chlorite which can easily be cleaved upon shear stress or by the peak stress at a crack tip because just weak van der Waals forces are acting between adjacent silicate layers (fig. 4).

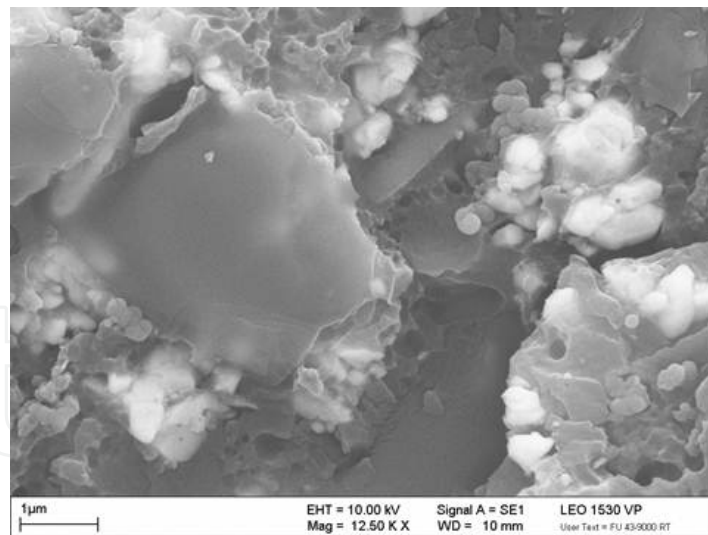


Figure 4. SEM picture shows a section of an impact crater. Smoothly cleaved talc particles led to cohesive failure of the conventionally pigmented automotive primer layer. Smaller white particles refer to titania, barite and calcite. Scale bar is 1 µm.

The physico-chemical principles described so far are all related to the properties of the solid coating layers. However with respect to the coatings design outlined in chapter 3 it has to be noted that the liquid coating materials – except for the ED coating which is exclusively a waterborne system – may either be solvent or water based. Whereas the vast majority of top

clear coat materials still is based on organic polymer solutions (plus cross linker and additives) the base coat and the primer are increasingly formulated as aqueous coatings in order to minimize the amounts of volatile organic compounds and thus fulfilling ecological and environmental regulations. However the notion “aqueous” implies that such formulations still comprise certain levels of organic solvents which by the majority are partly or completely miscible with water at ambient conditions.

2.4. Metal corrosion

Metal corrosion results from a redox reaction system constituted by three elements: an anodic site with an excess of electrons produced by the release of an equivalent amount of metal cations into the environment (= metal oxidation), a cathode where electrons are reducing either ions or water (reactants being O_2 , H_2O or H^+) thus releasing the corresponding reaction products like hydroxyl ions or molecular hydrogen respectively and an electrolyte as a conductive medium that enables an ionic current to flow thus ensuring electrical short-cut and a charge balance (fig. 5). The simultaneous presence of all three components and a perpetuate supply of the reactants is needed to maintain the currents and to degrade the anode material. Corrosion protection of non noble metal substrates requires that at least one of these elements becomes inhibited or at least significantly retarded. Active corrosion inhibition implies that a component from the environment (electrolyte, pretreatment, coating) interacts either with the substrate, the metal cations or the reduction products and that the reaction product forms an insoluble, stable layer or a deposit which impedes a further reaction at the respective electrode(s). On the contrary passive corrosion inhibition denotes the function of an applied coating to provide an effective diffusion barrier against water and ions from the environment thus isolating the corrosion sites from the electrolyte or retarding the formation of effective ion conductivity respectively.

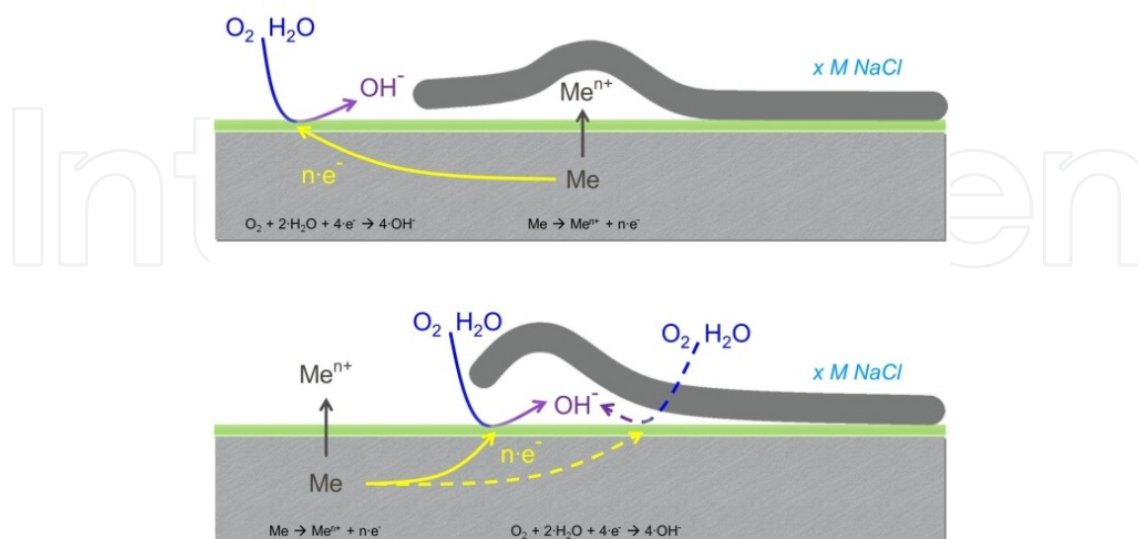


Figure 5. Anodic and cathodic corrosion process at defects on coated metal substrate (the green line symbolizes a conversion layer). Reaction of Me^{n+} with water may lead to precipitation of $Me(OH)_n$ and a local decrease of the pH value

There exist numerous techniques which have been used to investigate the electrochemical reactions occurring in the course of corrosion as well as to follow changes of the electrical resistance of a coated substrate. These analytical probes enable to determine electrochemical characteristics like the corrosion potential (E_{corr}), the corrosion current density (I_{corr}), the polarization resistance (R_p), the electrochemical noise resistance (R_n), the open circuit potential (E_{ocv}) by either polarizing the system (DC polarization, cyclic voltammetry), recording current and voltage fluctuations between two samples (electrochemical noise) or by following an open circuit potential of an immersed sample while the electrolyte is changed. Changing environmental conditions as well as progressing corrosion processes also alter the complex electrical resistivity of a coated sample which can be monitored with the electrochemical impedance spectroscopy which indirectly allows insights related to the evolution of the coatings barrier and self-healing properties or of the destabilization of the substrate coating interface. The locally resolved monitoring of corrosion allows the Scanning Vibrating Electrode Technique (SVET) by detecting gradients of the corrosion potential at the metal surface exposed to the corrosive medium. Similarly the Scanning Kelvin Probe (SKP) measures electrode potentials non-destructively at buried interfaces of a coated metal substrate and additionally displays the topography of the samples surface.

By coupling electrochemical techniques with chemical analysis of dissolved species within the electrolyte using e.g. ICP and / or the chemical nature of the exposed substrates surface during and after the exposure further valuable insights into the corrosion mechanism especially the role of the involved layers as well as the corrosion products can be obtained (Volovitch et al., 2011). Thus it could in principle be possible to quantitatively link stoichiometry (ratio of transferred electrons to converted chemical species) with corrosion rates.

Other tests evaluate and rate the corrosion resistance of coated samples by visual inspection of coated and in most cases marred (= scribed or stone impacted) specimen after an exposure to aggressive environments, either natural ones (e.g. maritime locations, industrialized districts) or artificial set-ups, the latter known as accelerated tests that are described by detailed protocols.

2.5. Corrosion protection

In the automotive industry the metals that are used for the manufacturing of the body or the body panels and framework reflect a vast variety of approaches towards lightweight construction, safety enhancement as well as an increased degree of freedom in the automotive design. Thus a broad variety of different metals and intermetallic alloys have been developed based on steel, zinc coated steel, aluminium and magnesium.

Most natural oxide or oxide-hydroxide passivation layers at the surface of these metals or alloys do not exhibit a sufficient resistance towards chemical degradation under those harsh environmental conditions often formed in the course of the corrosion processes. Another aspect is the fact that even the surface of a metal substrate consisting of only one single metal does not present a chemically homogeneous surface. First the solidification of the

metal melt in the course of the substrates manufacturing proceeds via a seed growth mechanism yielding a final patchwork of metal grains separated by grain boundaries. Second the crystallized grains may expose different crystal planes with respect to their topological *hkl* systematic towards the surface as well as at defect structures and grain boundaries. These normally translate into different topological crystal planes of the oxide passivation layer. The different crystal planes expose a different metal coordination chemistry and hence a different chemical reactivity to the surface. Although not yet scaled to industrial processes a recently published approach proposes a pretreatment process that addresses the grain boundary selective deposition of polymer colloids from aqueous solutions on zinc coated and acid activated steel panels (Hintze-Bruening et al., 2011). The stabilizing anionic groups of the particles complex metal ions liberated from anodic reactions. Their concentration varies locally being highest in the vicinity of the grain boundaries thus yielding to a local selective destabilization and deposition of the polymer particles.

Another aspect relevant to corrosion protection stems from the fact that nearly every thick organic coating system may comprises some flaws like pores, pinholes and cracks on the micrometer scale as well as a locally varying cross-link density in the case of reactive systems. Additionally in highly filled pigmented coatings diffusion channels for aqueous solutions might be present, e.g. along polar interfaces or electric double layers at the surface of percolating pigment or filler particles, as well as capillary forces. Thus, before applying such coatings the metal surface or the passivation layer should be treated or replaced respectively in order to obtain a thin stable layer on the nano- to micro-meter scale, the conversion coating. These are formed on the substrates surface via a “pretreatment”, a coating process normally comprising the cleansing (e.g. degreasing), an activation step (e.g. chemical dissolution to remove the native passivation layer) and finally the deposition of the conversion layer. As described above the common principle is to better protect the bare metal substrate against corrosion. However in many cases the conversion layer also provides a less polar and less smooth surface as the pristine substrate which in turn facilitates the adhesion of subsequently applied organic coating layers, either via mechanical anchoring or by specific molecular interactions or by both phenomena. Thus the bonderizing also known as phosphatization of steel and zinc coated steel comprises the precipitation of transition metal phosphates, e.g. the trication phosphatization forms zinc, nickel and manganese phosphates. These grow as coarse randomly oriented platelets from the metal surface leaving sufficient uncovered metal areas to ensure the electric conductivity which is needed for the cathodic reaction to take place in the subsequently applied cathodic electrodeposition paint process.³ Indeed for this still most abundant metal substrate of automotive manufacturing the combined bonderizing and cathodic electrodeposition coating has become a mature effective corrosion preventing technology which is inter alia reflected in ever increasing time limits of the warranty issued by the car manufactures.

³ The formed hydroxyl anions neutralize the organic acids that have been used for the formation of ammonium cationic groups by neutralizing tertiary amine bearing epoxy polymers. Hence the latter lose their colloidal stability and precipitate onto the metal surface of the automotive body. Aromatic moieties within the polymer backbone are supposed to interact effectively with the metal surface.

Such pretreatment may take place either as a continuous process in a coil coating line (e.g. zinc coating on steel, the passivation of aluminium with chromates) or subsequently on individual body panels or of the assembled automotive body respectively.

For nearly all other metal substrates but particularly for aluminium based parts the most effective corrosion inhibition system in the past was based on chromium associated in its hexavalent oxidation state (Cr^{6+}), the active species CrO_4^{2-} being slowly liberated from essentially insoluble strontium or barium salts up to their solubility limit under humid conditions, e.g. a coatings defect or water saturated coating. In the case of a starting corrosion process an insoluble and adherent layer of prevalently trivalent chromium comprising hydroxide forms on the substrate surface. Due to matching lattice parameters and the dielectric nature of the hydroxide layer both further metal dissolution as well as the cathodic reactions are effectively inhibited. However due its carcinogenic potential and environmental impact the use of this passivation has been banned by the Directive 2000/53/EC of the European Parliament and the Council of September 18, 2000. Therefore the development of chromate-free anti-corrosion coatings has become an ever growing research topic. Basically relying on the same principle, namely the slow release of oxoanions near a coatings damage and precipitation of a passivation or barrier layer as is the case of chromate and phosphate for aluminium and steel respectively, recent approaches to provide chromate substitutes have been introduced as “self-healing” concepts comprising the triggered release of corrosion inhibiting agents from depots imparted in the coating system.

2.6. Self-healing concepts

In the recent past the investigation of self-healing coatings has gained considerable attraction and even government-funded joint research initiatives like the European MUST program have been installed in order to provide the basis for future technical solutions. Common to all is the notion to furnish a coating system with depots of chemical active compounds which are released upon either a physical impact like mechanical stress, temperature or UV light or a chemical stimulus like a change of the pH value of the surrounding or the exposure to other species like water or ions. The chemicals imparted within the depots might either be active corrosion inhibiting compounds (e.g. ligands for substrate metals, precursor for passivation layers) or chemical reactants like monomers optionally along with cross-linkers or initiators which are thought to refill a void in the coating layer formed upon e.g. mechanical impact. However concerning the design of the host material a plethora of different approaches have been proposed. They span from sol-gel chemistry over micellar particles, Pickering particles, hard polymer capsules, sand-wiched shells of oppositely charged polyelectrolytes, porous minerals or oxides, tubular and layered clay minerals to hierarchically assembled frameworks. Regarding the different length scales covered as well as the different chemical stabilities of these materials it is obvious that some of these host architectures may be prone to different or even complementary trigger for release than others (e.g. hard polymer versus polyelectrolyte based capsules) or may provide additional benefits like an efficient diffusion barrier as it is the case of layered clay particles (table 1).

System / Trigger	Cl ⁻	Δ pH	H ₂ O	Δ T	mech.	light	chem.
no host							
sol-gel							
layered particles							
rigid polymers							
polyelectrolytes							
micelles							
Pickering particles							
hierarchical							

Table 1. Encapsulation systems and responsiveness towards stimuli compared to the direct addition of the inhibitor species into the matrix (= no host). This survey is loosely based on: Hughes et al., 2010.

In terms of container geometry the prevalent conception comprised discrete capsules dispersed in a polymer matrix. However with respect to rather thin layers in automotive coatings the overall dimensions of such depots and thus the amount of releasable components is very limited. Less relevant for corrosion inhibiting species which have to address a limited and in most cases moving interface or surface this aspect in particular affects the potential use for the self-repair of voids especially if larger defects from stone chipping are considered. In this context other coatings morphologies might be worth to be pursued where the depot extends over – theoretically – the whole coatings volume, e.g. by micro vascular networks which could either supply larger amounts of the repair system to one location or smaller amounts to the very same location if it comes to repeated damage. Filled fibres (Pang & Bond, 2005) and micro lithographic techniques (Toohey et al., 2009) have been proposed for the realization of such extended reservoirs in coatings.

Other self-repair systems target the curability (mendability) of smaller defects like fissures and cracks while maintaining an in principle cross-linked material via “photo-plasticity”. This concept implies the presence of photoactive polymer groups which – attached to the polymer backbone – might cleave upon UV exposure, rearrange and form new covalent bonds with other “dangling” reactive polymer ends or side groups. This can also be coupled with other functional groups attached to the polymer chains which are prone to mechanical stress and yield reactive groups complementary to those from the photo induced scission (Gosh & Urban, 2009). Such photoactive systems could react to tiny fissures that are formed within the organic coating due to residual stress present from the coatings processing in combination with a stress build-up over time via e.g. cyclic exposure to different environments with respect to temperature, humidity, chemicals and UV radiation⁴. Regular exposure of an automotive to sunlight thus could help to maintain the coatings barrier function over time by impeding the formation of larger crack or fracture.

⁴ Shorter wave length UV radiation is known to induce the formation of radicals as well as aggressive oxygen species (O₃, ¹O₂) that trigger cascades of reactions leading to cross linking as well as chain scission. Hence embrittlement as well as polymer degradation may occur contemporaneously and/or successively and optionally spatially separated depending on the formulation, physical properties and morphology as well as exposure parameters.

Within the present chapter we will in the following focus on the aspect self-healing of active electrochemical sites on the substrate by using lateral extended inorganic particles capable to form nano composites as well as to release active corrosion inhibiting species via ion exchange.

2.7. Polymer nano composites

Following pioneering research on clay-organic intercalates (Lagaly et al., 1973, 1975; Lagaly, 1981) it was in the late 1980s that Toyota's R&D work on Montmorillonite polyamide composites (Fukushima et al., 1988) triggered extensive research and application related work in the field of polymer intercalated and exfoliated layered particles. The morphologies compared to a composite comprising the aggregated counterpart are shown in figure 6. These were supposed to impart strength and thermal stability as well as a diffusion barrier to the polymer at comparatively low loadings with the inorganic particles of 5 – 10 weight per cent. Consequently they have also been proposed as new materials for automotive applications, however not in the context of coatings (Garcés et al., 2000). The vast majority of composites have been based on Smectite clays and Montmorillonite in particular. Each platelet of this natural clay that is essentially constituting the mineral Bentonite consists of a central layer of aluminium and magnesium cations octahedral coordinated with hydroxyl anions covered on both sides by a layer of silica tetrahedrons: $\{Al_{1.67}Mg_{0.33}(OH)_2[Si_4O_{10}]\}$. The net negative charge of the overall structure which is equivalent to the proportion of Mg(II) in the central layer is compensated by cations like sodium or calcium that are intercalated. Typical charge densities are in the order of 100 meq/100g and the lateral dimensions of the 1 nm thick platelets vary between several hundred nanometers and one micrometer. Such a polar, charged stacking readily incorporates water molecules. Therefore the interlayer distance which is in the order of one nanometer depends on the level of environmental humidity. Additionally natural intercalated cations may easily be exchanged by organic cations like quarternized fatty acid derived amines. Indeed "organo-clays" have been the workhorse for the preparation of polmer nano-composites in most cases due to a given tunable compatibility with organic hydrocarbon based structures and an increased interlayer distance. Methods comprise in-situ polymerization, solution blending (polymer is dissolved in solvent) as well as polymer melt processing. Besides rendering polar clay

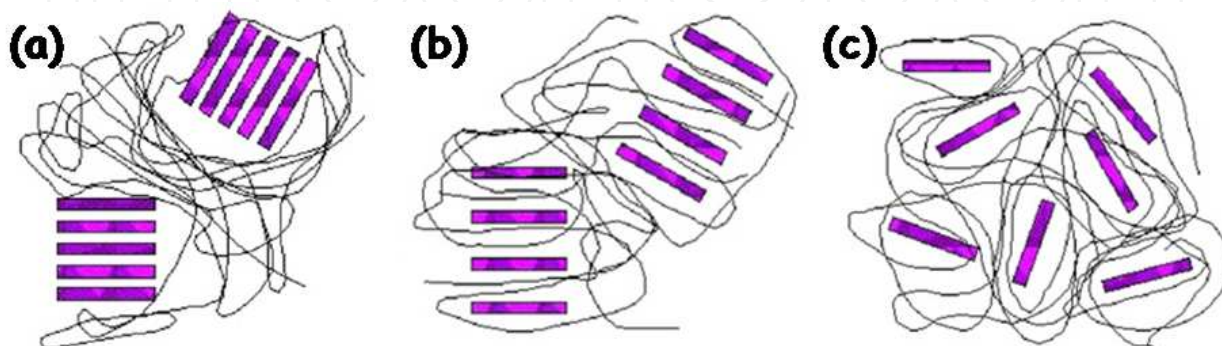


Figure 6. Aggregated (a), intercalated (b) and exfoliated (c) structures for nano composite materials based on layered fillers dispersed in polymer matrices.

“organophilic” reactive clays have been proposed for numerous in-situ polymerization systems, e.g. of epoxy resins via acidic ammonium (Lan et al., 1996), lactone via transition metal compound (Lepoittevin et al., 2002) or in combination with radically polymerized olefinic unsaturated monomers (Di & Sogah, 2006). Other approaches make use of pristine clays in heterophase polymerizations, either emulsion polymerization (Huang & Brittain, 2001) or mini emulsion polymerization (Cauvin et al., 2005), where the mineral platelets are found at the interface between the aqueous phase and the polymer particles to yield Pickering like armored particles.

Regarding the mechanical properties the stiffening effect of intercalated and to some extent exfoliated composites has been attributed to an immobilization of the polymer matrix. Thus polymer chains confined within the platelets interstitial space or tethered to the platelets surface may extend into the surrounding matrix and entangle with each other (Rao & Pochan, 2007). Hence the effective volume of the platelets exceeds that of the neat particles. Consequently a huge effect in the mechanical response to external stress can be observed as reinforcement accompanied with a decrease of polymer chain flexibility expressed as a reduced loss modulus in dynamic mechanical analysis. Obviously the stress transfer over the volume of a work piece scales with the platelets aspect ratio and from theoretical considerations as well as from biological systems it is known that the probability to dramatic failure due to flaws inversely scales with the thickness of the particles (Gao et al., 2003). However numerous studies have shown that polymer clay nano composites tend to show brittle failure in impact tests or to provide a reduced toughness in tensile tests in comparison with the unfilled polymers. Reasons might be local stress build up and thus crack initiation at aggregated inclusions. However in first instance it is due to the particles restricted mobility in a glassy matrix system. By shifting the time-temperature parameter frame of the test method relative to the glass temperature of the polymer a shift from brittle to tough failure can be observed (Shah et al., 2005). This was corroborated by simulation results which show that the particles mobility in the matrix is a decisive prerequisite for tough failure (Gersappe, 2002). In semi-crystalline polymer systems the nano-particles impact on the crystallization of the polymer phase was also shown to dramatically increase the failure toughness by changing the overall matrix morphology (Shah et al., 2004).

With respect to the diffusion barrier of clay based composites this is mainly attributed to the tortuosity for the diffusing species (Triantafyllidis et al., 2006). It was particularly shown that penetration rates inversely scale with the aspect ratio of the clay platelets (Gatos & Karger-Kocsis, 2007; Kugge et al., 2011).

3. Layered Double Hydroxide – Polymer composite based coatings

3.1. Layered Double Hydroxides (LDH)

LDH structure is described with the ideal formula, $[M^{II}_x M^{III}_{1-x} (OH)_2]_{intra} [A^{m-}_{x/m} \cdot nH_2O]_{inter}$, where M^{II} and M^{III} are metal cations, A the anions and *intra* and *inter* denote the intralayer domain and the interlayer space, respectively. The structure deviates from the layered morphology of magnesium hydroxide (Brucite, $Mg(OH)_2$) – consisting in edge sharing

octahedrons of hydroxyl anion coordinated metal cations. Compared to the neutral brucite framework, partial M^{II} to M^{III} substitution induces a positive charge for the layers, counterbalanced with the presence of the interlayered anions. Edge sharing $M(OH)_6$ octahedra yield inorganic sheets in the lateral dimension while the anions induce a stacking of the sheets as illustrated in Fig. 7. Structurally, polytypes based on two-, three- and six-layer polytypes presenting either rhombohedral (2R, 3R, 6R) or hexagonal symmetry (2H, 3H, 6H) are determined from the powder X-ray diffraction diagrams (Bookin et al., 1993). However the LDH and the hybrid derivative materials are usually poorly crystallized and the more common three-layer polytype 3R₁ with rhombohedral symmetry (space group R-3m) is often adopted. From a long range order, the stacking of LDH sheets is viewed as layers translation of $(2/3a + 1/3b)$ between consecutive layers.

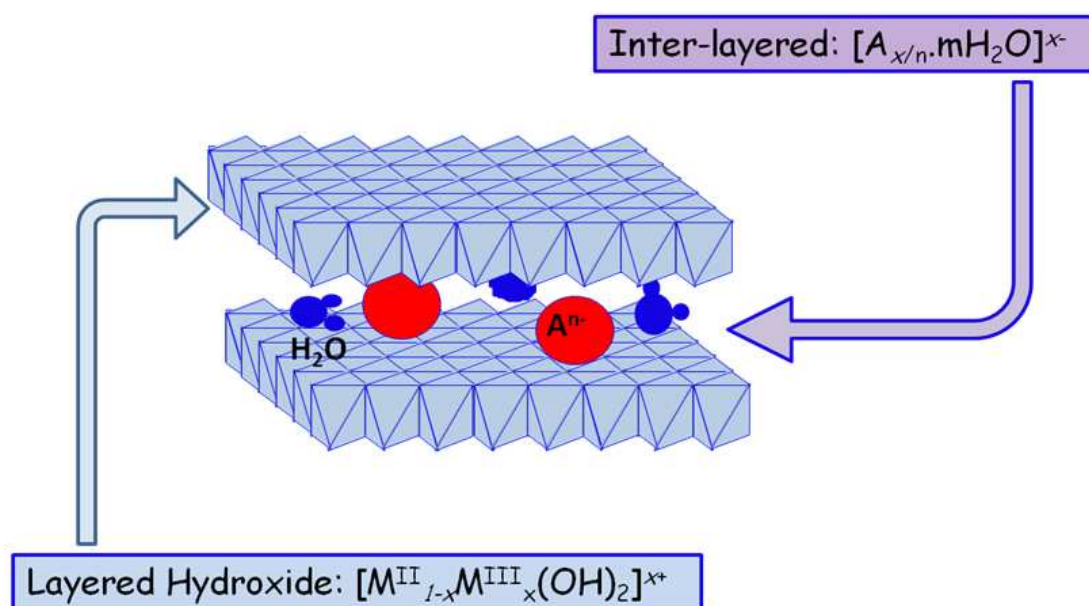


Figure 7. Structure of Layered Double Hydroxide material

In term of crystal identification and natural abundance, hydrotalcite of composition $Mg_6Al_2(OH)_{16}(CO_3) \cdot 4H_2O$ was first identified in Sweden in the year 1842. Many other minerals presenting different chemical natures are belonging to this large family, such as manasseite, $Mg_3Al(OH)_8(CO_3)_{0.5} \cdot 2H_2O$, meixnerite, $Mg_3Al(OH)_8(CO_3)_{0.5} \cdot 2H_2O$, sjögrenite $Mg_3Fe(OH)_8(CO_3)_{0.5} \cdot 2.25H_2O$, stichtite, $Mg_3Cr(OH)_8(CO_3)_{0.5} \cdot 2H_2O$, takovite $Ni_3Al(OH)_8(CO_3)_{0.5} \cdot 2H_2O$, pyroaurite, $Mg_3Fe(OH)_8(CO_3)_{0.5} \cdot 2.25H_2O$, wermlandite, $Mg(Al,Fe)_{0.5}SO_4 \cdot 2H_2O$, hydrocalumite, $Ca_2Al(OH)_6(CO_3)_{0.11}(OH)_{0.78} \cdot 2.38H_2O$, $Fe^{II}_4Fe^{III}_2(OH)_{12}SO_4 \cdot nH_2O$, an iron hydroxysulphate commonly called greenrust, and others. Naturally not abundant, synthetic LDH materials nowadays are, however, produced in relative large amounts, this promoted by a high global demand of their use in ethanol steam reforming, biodiesel production and in plastics processing industry to replace heavy-metal additives for PVC as well as bromide-based fire retardants in other polymers.

Simple, reproducible and rather inexpensive syntheses have been developed to produce LDH materials. The co-precipitation process at a fixed pH value is largely employed to

yield materials with chemical homogeneity. Standard LDH products bearing anions such as nitrate or chloride may subsequently be used to yield LDH phases comprising other anion compositions through ion exchange topotactic reaction. Other procedures such as metal salt and metal oxide addition and reconstruction from amorphous calcined LDH precursors yield materials of lower crystallinity and potentially accompanied with non LDH phases. During a co-precipitation both nucleation and growth process steps occur simultaneously, resulting in particles presenting a relative broad size distribution. Size distribution may be limited at the expense of a lower crystallinity by using short addition times and by avoiding any ageing step after the co-precipitation. For a better control of the particle size distribution, a rapid coprecipitation reaction is associated either to a separate aging step (Zhao et al., 2002) or to a subsequent controlled hydrothermal treatment (Xu et al. 2006), both methods yielding stable homogenous LDH suspensions with controllable particle sizes of interest for the elaboration of thin films or nanostructured materials. Another option is the so called “homogeneous precipitation” through urea hydrolysis and decomposition at slightly elevated temperatures (Ogawa & Kaiho, 2002). Urea decomposes into ammonium cyanate and successively into ammonium carbonate and ammonia upon hydrolysis, the rising pH value provokes the precipitation of the metal salts yielding micrometre sized, monodisperse and well-shaped carbonate bearing LDH particles.

Aqueous medium is largely preferred for the coprecipitation process, but other solvents maybe employed. For instance the polyol method performed by the hydrolysis of the metal acetate salts in ethylene glycol or di ethylene glycol under heating produces pure acetate intercalated LDH, this in absence of pH and atmosphere control and without an excess of a base (Prevot et al., 2005). Alternatively the sol-gel route in an organic medium yields LDH materials after hydrolysis and condensation polymerization reactions of metal alkoxide precursors (Wang et al., 1999). Of lower relevance for large scale production and from application related aspects, reversed micelles or micro emulsions may be employed to drastically change the LDH platelets morphology into fiber-like particles (Hu & O'Hare, 2005), and a sophisticated method using inverse opals is reported to yield three dimensional ordered macroporous LDH materials, the polystyrene beads based opal array acting as a sacrificial template (Géraud et al., 2006).

As evidenced from the natural occurrence, the chemical variety of hydrotalcite class of materials is rooted in a broad range of compositional tolerance with respect to the nature and ratio of divalent and trivalent cations according to their associated oxidation state and ionic radius as well as from the nature of the interleaved anion. The ratio of divalent and trivalent cations induces a net positive charge layer, resulting in a variable of interleaved anions. The anionic exchange capacity usually ranges between 450 to 200 meq/100 mg that corresponds to an average area per charge between 25 and 40 Å²/e⁻. It is importance to tune the platelets interface in order to enable the accommodation of cumbersome guest molecules as such high charge densities picture layers that are tightly stacked by electrostatic attraction

translated via the interlayer anions and / or by attractive forces acting laterally between the densely stacked anions. Indeed the usual $M^{II}M^{III}$ cation repartition results in LDH stacking being reluctant to exfoliate. However stable colloidal suspensions of exfoliated platelets can be obtained by the use of specific solvents such as formamide in addition to ultrasound for nitrate-based LDH (Liu et al., 2006), *N,N*-dimethylformamide-ethanol for carbonate-based LDH (Okamoto et al., 2006) or even water for alkoxide (Gurski et al., 2006) or lactate (Hibino & Kobayashi, 2005) intercalated LDH. It was observed that LDH nano sheets gradually dissolve in organic solvents.

With regard to their size – whether atomic or polymeric – and their valence from one to polyvalent a vast variety of species can be intercalated and exchanged by others depending on their characteristics. However driven by the intense research devoted to polymer-clay nanocomposite (PCN) (see section 2.7), surfactant molecules are commonly used to render the LDH sheets organophilic. It is comparable to the lipophilization of the smectite-type clays by alkyl ammonium cation to reduce the surface polarity of the silicate layers, and thus to supply a satisfactory affinity between them and a polymer. Another aspect is to consider LDH open-structure as an available container to embark and deliver functional species. This aspect is developed in more detail in section 3.3.

In addition to the tunable intra- and inter- chemical composition that permits to adapt LDH platelets for multiple applications and specific requirements (ecology, toxicity, functionality) bi-dimensional assembly of LDH platelets presents mesophasic ordering in suspension and in bulk polymer. Evidenced by birefringence observation, colloidal platelets of LDH show isotropic (I) to nematic (N) phase transition as a function of the concentration (Zhang et al., 2007). However high platelets concentration as high as 20% (wt.wt.) is needed to realize the I-N phase transition with the co-existence of a sol-gel transition. At lower concentrations in toluene I-N transition was observed with LDH platelets grafted with amino-modified polyisobutylene (Mourad et al., 2008) as well as with LDH particles dispersed in high-molecular weight polyvinylpyrrolidone (Luan et al., 2009). More recently the possibility to use such organized hierarchy was applied to polymer coatings (Troutier-Thuilliez et al., 2011), more developed in section 3.2.

Another interesting aspect for the application of LDH in coatings is their ability to arrange themselves in the form of thin films on a (metal) substrate or to be generated onto a metal substrate. Academically the formation of M^{II} -Al- NO_3 LDH films is reported on the surface of Al_2O_3 (Paulhiac & Clause, 1993) when contacting with M^{II} (M^{II} = Zn, Mg, Co and Ni). Optimized adsorption onto Al_2O_3 surface arises near its isoelectric point (i.e.p.) at pH 7.3 demonstrating that the formation of the LDH film proceeds by surface adsorption rather than electrostatic impregnation. Onto Al metal substrate highly porous Zn-Al LDH films with thicknesses on several micrometers are grown by reacting zinc salts and ammonia (Gao et al., 2006), while Zincite (ZnO) precipitates onto Al-free surfaces (Si, glass, plastic). The cross-section of a LDH film obtained after 12h at 50°C using a NH_3 to Zn ratio of three is shown in figure 8.

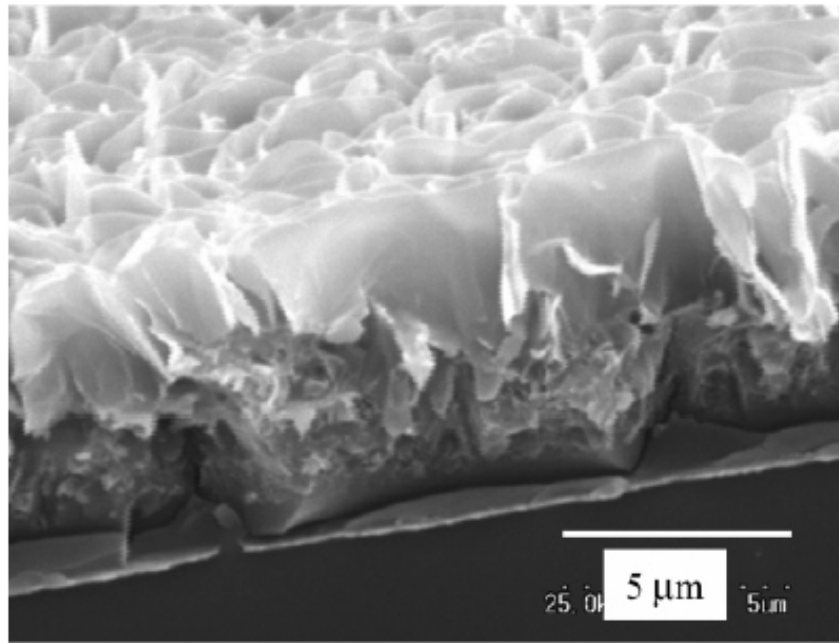


Figure 8. SEM images of LDH film grown on Al-bearing glass substrate after (Gao et al., 2006).

Alternatively this technology appears appealing to protect Mg and Zn rich alloy substrates. The combined deposition of LDH with surfactants yields superhydrophobic barrier films that are of interest in coatings science (Chen et al., 2006). Finally thin and ultrathin LDH films have been developed for energy management, thus via electrodeposition highly exposed electrode materials can be prepared (Gupta et al., 2008). For instance Ni or Co LDH films are cathodically electrodeposited through the reduction of nitrate ions; the increasing OH^- concentration promoting the LDH precipitation at the surface (Indira & Kamath, 1994). However published work on electrodeposition on the laboratory scale suggests that this method shall be deemed to be challenging to scale-up due to the observed vulnerability of the coatings to form defects like cracks and uncovered domains despite carefully controlled parameters (current density, concentration, time, temperature).

3.2. Aqueous LDH based coatings

As outlined in chapter 2.2 automotive primers for instance are based on tough polymers capable to form hydrogen bonds (e.g. polyurethanes) that are highly filled with inorganic micron-sized particles like titania, barite, and easily cleavable talc, which primarily cause cohesive failure of the coating upon impact. With respect to integrated coating systems (see chapter 2.1.) without such a primer layer the mechanical functionality should be imparted into the remaining coating layers which have to provide additional functionalities like colour effect (aesthetics) or corrosion inhibition (diffusion barrier, inhibitor release). Thus it would be highly desirable to increase the scope for formulation by reducing the amount of loading of the polymer phase with filler particles. One attractive strategy is the use of exfoliated as well as polymer intercalated layered inorganic particles which are known to reinforce polymer matrices at low loadings through coordinate stress transfer. As described in chapter 2.4. large aspect ratios of these particles are preferred in view of the mechanical properties. However

dimensions of up to several hundred nanometer surpass typical sizes of polymer colloidal particles that are in the order of 20 to 100 nm. Accordingly they usually have to be dispersed within the continuous aqueous phase of the liquid coating. In order to maintain a low initial as well as storage stable viscosity of this material allowing for spray application particle-particle interactions have to be controlled. This concerns in particular the interactions between the layered inorganic particles – thus the gel formation of quite diluted aqueous dispersions of phyllosilicates like Laponite and Montmorillonite resulting from the aggregation of clusters formed by exfoliated platelets or small staples of platelets has been a widely studied phenomenon (Mourchid et al., 1995; Dijkstra et al., 1997; Pignon et al., 1997; Shalkevich et al., 2007; Joensson et al., 2008; Cousin et al., 2009). Also specific interactions between polymers and the inorganic particles have to be considered (Balazs et al. 1998; Milczewska et al., 2003; Alemdar & Buetuen, 2004; Wang et al., 2006). In this respect combining oppositely charged components like positively charged platelets and anionic stabilized polymers or colloidal polymer particles appears to be adventurous regarding possible heterocoagulation as it was observed with oppositely charged inorganic particles (Ji et al., 2004). However within the following chapters it is shown that, within a given toolbox of waterborne polymer colloids, water soluble polymers and water dispersible LDH particles, by tuning the compatibility between the polymers as well as the interfacial properties between the polymers and the LDH particles, storage stable aqueous coating materials can be formulated. Furthermore upon spray application and film formation of several of these formulations a broad range of different coatings morphologies – all providing excellent impact resistance – are obtained.

3.2.1. *Intrinsically incompatible matrix*

For stone impact resistant coatings, dispersed soft phases, in particular bicontinuous phases, have been claimed, since heterogeneous (polymer) film morphologies are known to be beneficial for stress relaxation and for the limitation of unstable crack growth as outlined in section 2.2. In this context, a ternary composition was designed, comprising polyester (PES), blocked polyiso-cyanate (PURx) and hydrophobic polyurethane (PURh) (Hintze-Bruening et al., 2009). It has to be emphasized that contrary to the crystalline LDH phases, the polymers both of the reference system and of the mixtures described in this and the following sections are technical, structurally non uniform products with rather broad molecular weight distributions obtained from step growth polymerizations. However as visualized by CLSM using fluorescent labeled versions of PES and PURh, the mixture shows a spinodal like polymer phase separation upon water flash off. This produces a heterogeneous film structure in the baked coating with large dispersed areas of a less dense phase which primarily is constituted by PURh.

In the presence of the carbonate (CO_3^{2-}) and 4-amino benzene sulfonate (4-ABSA) comprising $\text{Zn}_2\text{Al}(\text{OH})_6$ LDH particles, the phase separation becomes either retarded or accelerated, respectively, as was deduced from the resulting film morphologies. With the organic modified particles, a dispersed softer PURh phase of significant smaller droplet size was found within a continuous more rigid and elastic composite phase. Morphologies where both phases are continuous were also obtained using LDH particles with smaller lateral dimensions, as with the 3-ABSA intercalated $\text{Mg}_2\text{Al}(\text{OH})_6$ phase (Fig. 9).

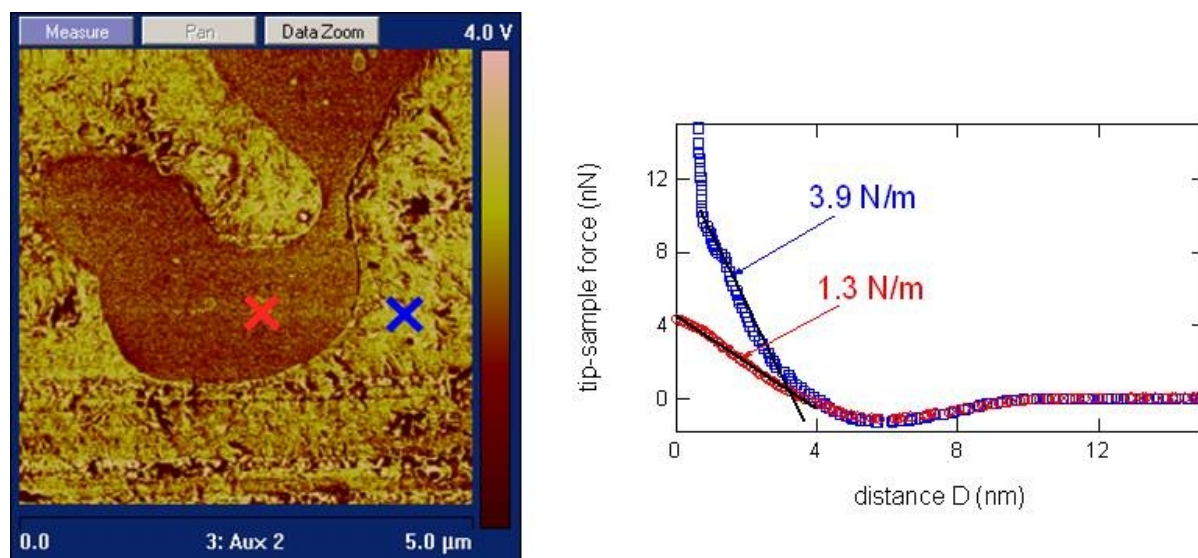


Figure 9. Multiple heterogeneous morphology of a baked film comprising polymer intercalated $\text{Mg}_2\text{Al}(\text{OH})_6 - 3\text{ABSA}$ as rigid phase (blue) besides PURh based soft phase (red). AFM phase contrast image ($5 \times 5 \mu\text{m}$) and force distance curves. The colour codes are also valid for Fig. 10.

It is conceivable that besides a positive impact of the particles on the viscosity development of the continuous polymer phase (as observed in the rheological behavior of a reference system, see below), the LDH particles might simply form physical obstacles for the moving interface between the demixing polymer phases. This latter effect was simulated for binary polymer systems comprising spherical hard particles (Ginzburg et al., 1999) and corroborating morphologies were observed with several silica beads filled (Karim et al., 1999) and smectite filled non crystalline polymer blends (Yurekli et al., 2003, 2004). Indeed CLSM and XRD studies revealed that the PES (and possibly both the polar components PURx and MF resin) readily intercalates the LDH galleries in the initial waterborne coating material while the particular shape of the micron sized aggregates of polymer intercalated LDH particles slowly disappears during the air drying process. An inverse impact on the kinetics of the polymer phase separation was found with the carbonate bearing LDH particles which enables a stratification of the film where a continuous PURh layer covers a composite phase that comprises the aggregated, not polymer intercalated LDH particles. Due to their basic nature, it is conceivable that the carbonate bearing LDH particles retard the acid catalyzed transesterification of the melamine formaldehyde resin.⁵

It is noteworthy that the particle impact on the kinetics of the polymer phase separation follows the same trend which was observed for the viscosity development of a reference system that was based on an aqueous PUR dispersion (Troutier-Thuilliez et al., 2009). This commercial grade polymer was shown by XRD studies and TEM imaging to readily intercalate organic anion bearing LDH phases whereas no specific interactions and intimate blending occurs in the presence of the carbonate comprising LDH particles. However, the 4-ABSA anions render the LDH particles organophilic but still incompatible with the hydrophobic

⁵ Importantly, curing reactions are not generally be hampered by the presence of LDH phases as demonstrated with cross-linked polysiloxanes on a metal substrate (Kanai & Nomura, 2009) and in a sol-gel based coating (Alvarez et al., 2010).

polyurethane PURh of the ternary mixture which was demonstrated with another reference coating material that was exclusively based on PURh as the polymer part. This incompatibility might not be fully attributed to the hydrophobic nature of the polymer chains stemming from the incorporated dimer fatty acid moieties. This was shown with another LDH phase that beared intercalated fatty acid carboxylates (C12) instead of 4-ABSA. Although favourable interactions with the PURh chains are expected no intercalation could be observed. A possible explanation might be the lack in entropic gain. Assumed that the polymer intercalation proceeds via anion exchange the system would gain entropy by the released small anions 4-ABSA or dodecyl carboxylate. However due to distinct van der Waals attractions and as the conjugated base of a weak acid the latter are only slightly water soluble under ambient conditions.

As with the baked films of the reference system, typically stacks of tennish polymer intercalated and approximately 10-15 nm separated platelets of the initially 4-ABSA bearing LDH phase are found to be homogeneously and isotropically distributed throughout the continuous phase besides minor amounts of singular platelets and some stacks of platelets which retained their original interlayer distance. The stacks of polymer intercalated platelets or polymer separated stacks of non-intercalated platelets appear as alternating rigid soft layers which micromechanically could be considered as sliding planes in the case of shear stress and as springs or attenuators under compressive load. Additionally as described in section 2.7. and known in the context of smectite filled polymer system, the confinement of polymers strengthens the continuous polymer phase near and above the glass transition temperature. In combination with the presence of the dispersed soft PURh phase as well as the tortuous path for growing cracks these features were attributed to be the main causes for the excellent stone chip performance obtained with model automotive coatings comprising these materials as a primer layer which is visualized by the fracture surface that is shown in figure 10.

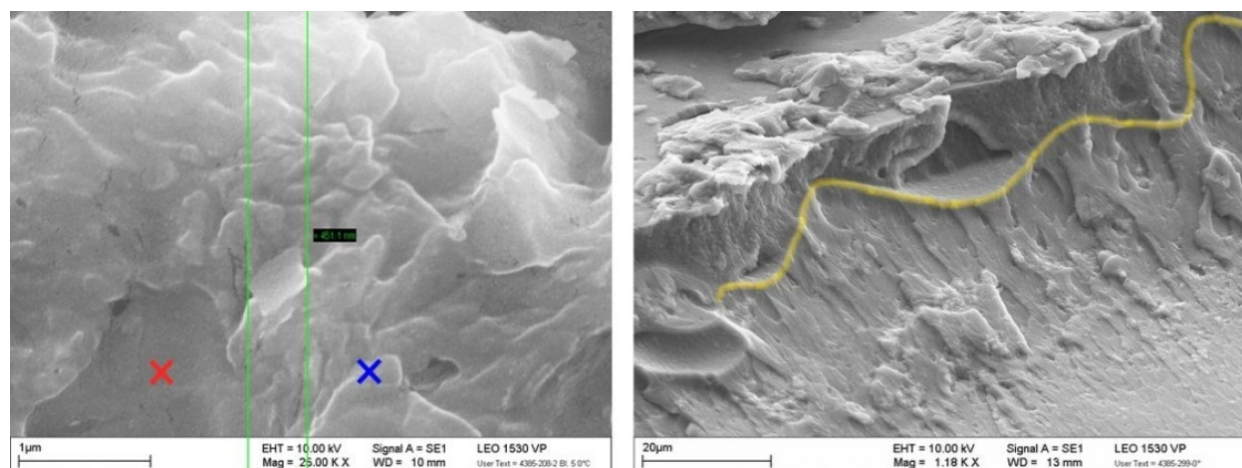


Figure 10. Sections of impact crater produced from single spherical impacts at 273K. Fracture surfaces of the primer layer are shown. Left image shows the composite of Fig. 9., scale bar is 1 μm. Tortuous cracking took place in the rigid composite leaving individual LDH stacks behind. Right image is a stratified primer (yellow line = interface) comprising aggregated carbonated LDH particles in the layer beneath the upper PURh phase, scale bar is 20 μm.

3.2.2. Compatible matrix & ordered films

Another approach to achieve high impact resistance in coatings could be the formation of textured composites including platelets that are aligned parallel to the substrate surface. Thus a high level of ordering at the scale of building blocks is reminiscent of bio-related frameworks, inspired by aragonite protein brick mortar assemblies found in e.g. nacre and reported in the literature as high strength materials. However these artificial materials are typically obtained by tedious application techniques, e.g. via layer by layer deposition that are economically unaffordable for industrial processing (Bonderer et al., 2008). In contrast LDH particle-based composites with distinctly oriented thin stacks of LDH platelets were obtained from a single application step of a $\text{Zn}_2\text{Al}(\text{OH})_6$ 4-ABSA LDH particle comprising aqueous binary mixture of compatible polymers (Hintze-Bruening et al., 2011). Both polymers exhibit some amphiphilic features by combining hydrophobic backbones with anionic stabilizing groups: a polyurethane (PURh)⁶ and a polyester (PESh).

It could be shown that the formation of this texture is due to some intermediate colloidal stage of a lyotropic liquid crystal like (LC) ordered liquid phase which arises from ionic interactions between protonated amino groups of 4-ABSA molecules on the LDH platelets surface and the carboxylate moieties of the PESH. Besides the well-known attempt of charged layered particles to gain entropy via reducing their excluded volume if dispersed in water, an additional enthalpy related driving force might be an effective lamellar shielding of the hydrophobic PESH backbone against the aqueous phase if adsorbed between adjacent LDH platelets. Thus a lamellar texture indicated by the fluorescent labelled PESH within an intermediate preparation stage of the coating was visualized with CLSM. Besides a nematic phase of poly(isobutylene) stabilized LDH particles in toluene (Mourad et al., 2008) a lyotropic mesophase of polymer stabilized LDH in water had not been described before.

Upon stirring the LDH particle slurry into the aqueous PESH dispersion, a stable viscous paste showing “schlieren” is obtained. These could be assigned to a nematic ordering as was shown by textural domains visible under cross polarized light as well as in cryo SEM pictures. Ultra small angle X-ray scattering (USAXS) confirms the mean spacing between the lamellae as observed in the cryo SEM picture by exhibiting a peak corresponding to a distance of 75 nm. Such a distance is not revealed by cryo TEM images of individual lamellae that are predominantly constituted by parallel aligned LDH platelets (Fig. 11). Despite their rather non-uniformly stacking in terms of the number as well as with regard to the interlayer distance of the individual LDH layers, this varying morphology still gives rise to distinct peaks in the SAXS curve over four harmonics corresponding to a mean spacing of 21 nm. The scattering intensity follows an $I(q) = q^{-2.01}$ power law decay which is that expected for individual platelets.

⁶ Note that the hydrophobic nature of the polymer backbones is stemming from dimerized fatty acid that is used as a monomer in the synthesis of the polyester intermediate polyols. With this respect PURh is similar to that PURh described in the preceding section, both only differing by the type of diisocyanate that was used for the polyaddition step in the synthesis of the polyurethanes.

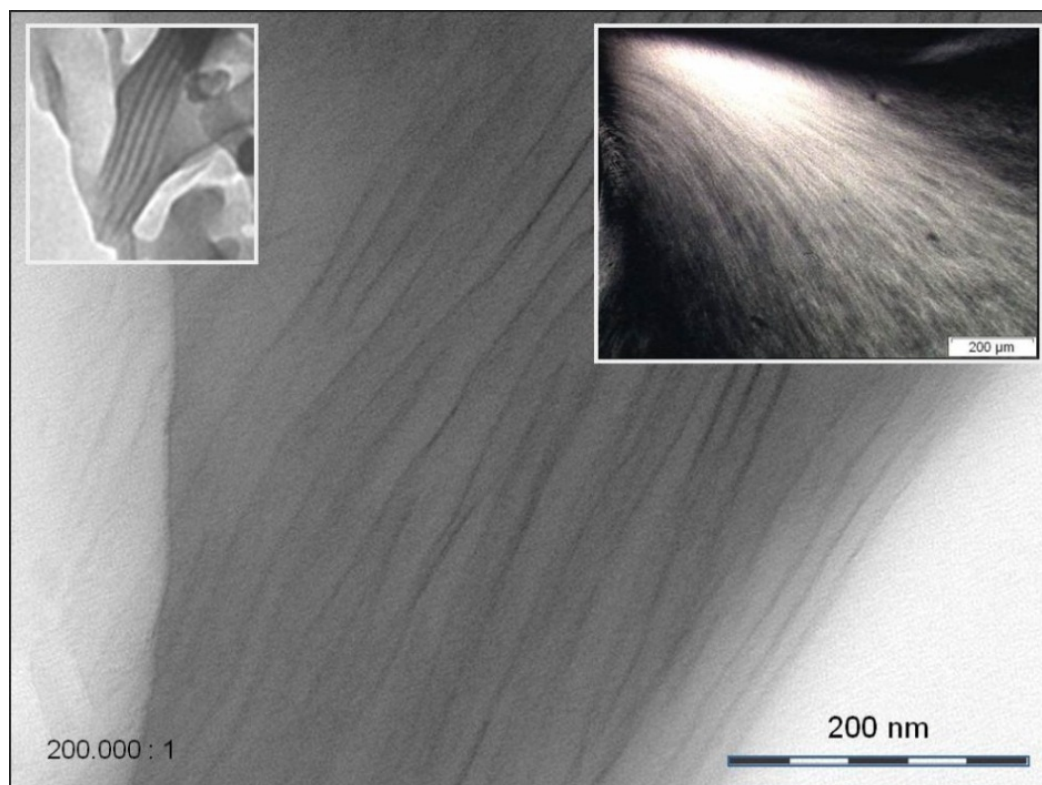


Figure 11. Cross polarized OM image (right insert, scale bar 200 μm) shows an ordered liquid composed of aligned lamellae (TEM image, left insert) which comprise irregularly parallel aligned individual LDH platelets with a mean spacing of 20 nm (cryo TEM images).

Combined with the aqueous PURh dispersion and the melamine formaldehyde resin (MF), smooth highly transparent films can be obtained after drying and baking.⁷ It could be shown that within the liquid coating material the ordered nematic like phase of the intermediate disrupts into micron sized fragments which are still constituted of LDH platelets separated by 20 nm according to cryo SEM images and peaks in the SAXS curve. These lamellar fragments still comprise the major portion of the PESH which was visualized by the fluorescent labelled polymer in confocal laser scanning microscopy (CLSM). The morphology of free films was investigated by TEM and XRD (Fig. 12).

The LDH platelets' interstitial space from the liquid coatings LDH bearing fragments has been compacting during film formation and baking yielding aligned tiny stacks with an interlayer spacing of 10 nm. These stacks comprise LDH platelets that are separated by 1.76 nm. The alignment parallel to the substrates surface is far from being perfect as revealed by stitched TEM pictures but essential enough to give rise to either the 003 or the 010 and 100 reflections in the SWAXS curves depending on the inclination angle of the specimen.

The small interstitial spacing of 1.76 nm corresponds to that of the pristine LDH phase bearing intercalated 4,ABSA anions. However these were found to be liberated from the intermediate PESH LDH preparation into the aqueous phase. Hence such a restacking would

⁷ The ordered nematic like liquid of the intermediate preparation does not yield a film. After drying and baking extended, quasi "bicontinuous" phases are found: a LDH rich solid phase besides a transparent LDH free polyester based (viscous resinous) phase.

be a remarkable finding and deserves further investigations as well as the role of the film forming polyurethane colloids. The latter was found to be incompatible with the (pristine) LDH phase like the one of the incompatible polymer system described in section 3.2.1.

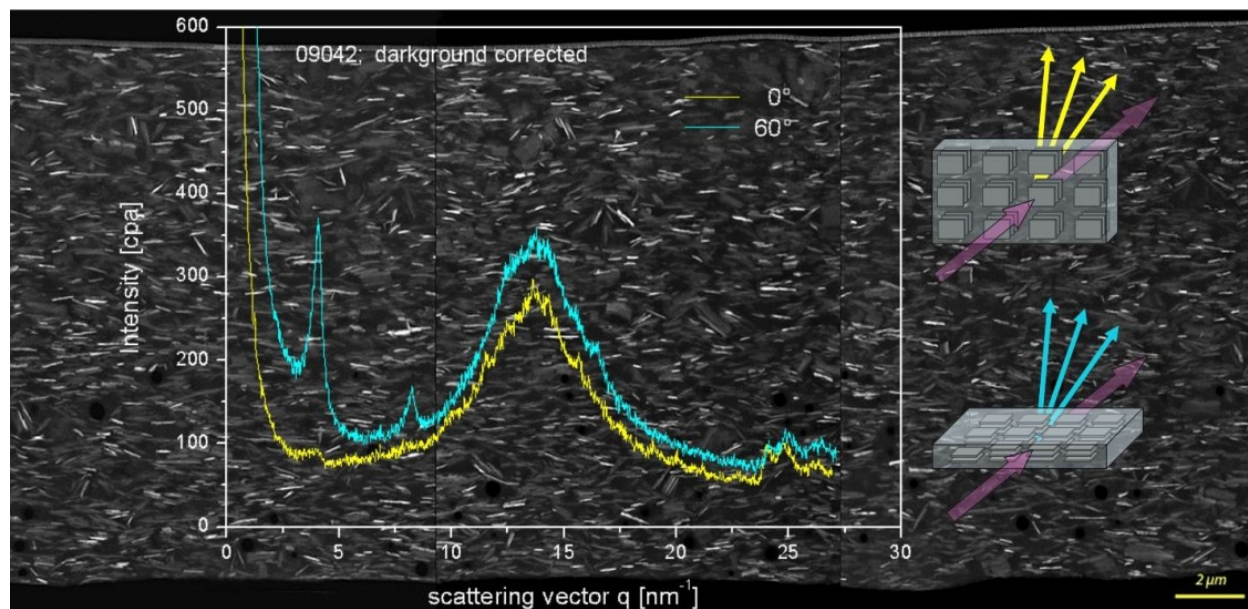


Figure 12. Stacked HAADF-TEM images and corresponding SWAXS diffraction curves from different inclination angles of a baked film of the aqueous, PURh diluted nematic like meso-phase of PESh stabilized LDH platelets. Black spheres with diameters of $\sim 1 \mu\text{m}$ in the lower part of the film are discussed in the text and emphasized in Fig. 13.

If such a liquid formulation of PURh fragmented ordered LDH – PESh intermediate liquids was sprayed as a primer layer in the same model automotive coating system already introduced in the preceding section an outstanding stone chip resistance was observed. SEM fracture analysis of an impact crater produced by a single spherical impact test that was applied on the very same test panel revealed that remnant substrate near pieces of the fractured layer expose – besides some LDH platelets – the replica of numerous spherical “inclusions” with a typical diameter of one micro-meter or less (Fig. 13).

These witness a foamy morphology of the lower part of the primer layer. The gaseous inclusions are also visible in the TEM image of the free film as dark spots and they are most probably constituted by either accumulated air from the application or (and) by liberated methanol from the trans-etherification cross linking reaction of the melamine formaldehyde resin. Thus the excellent impact resistance may not (exclusively) be attributed to the ordered LDH composite since a porous morphology is also known to be beneficial for stress dissipation and limitation of crack growth (see also sections 2.2 and 2.3). The use of breakable hollow spheres as filler particles for stone chip resistant coatings accordingly was an early proposal albeit studies were limited on systems comprising glass spheres on a much bigger length scale. In contrast the present model coating demonstrates the possibility of an in-situ formation of such porous structures on an appropriate scale by providing an efficient diffusion barrier within the coating layer. Such a combination of mechanical

performance and barrier properties might be the basis of multifunctional coatings in terms of corrosion protection of the metal substrate.

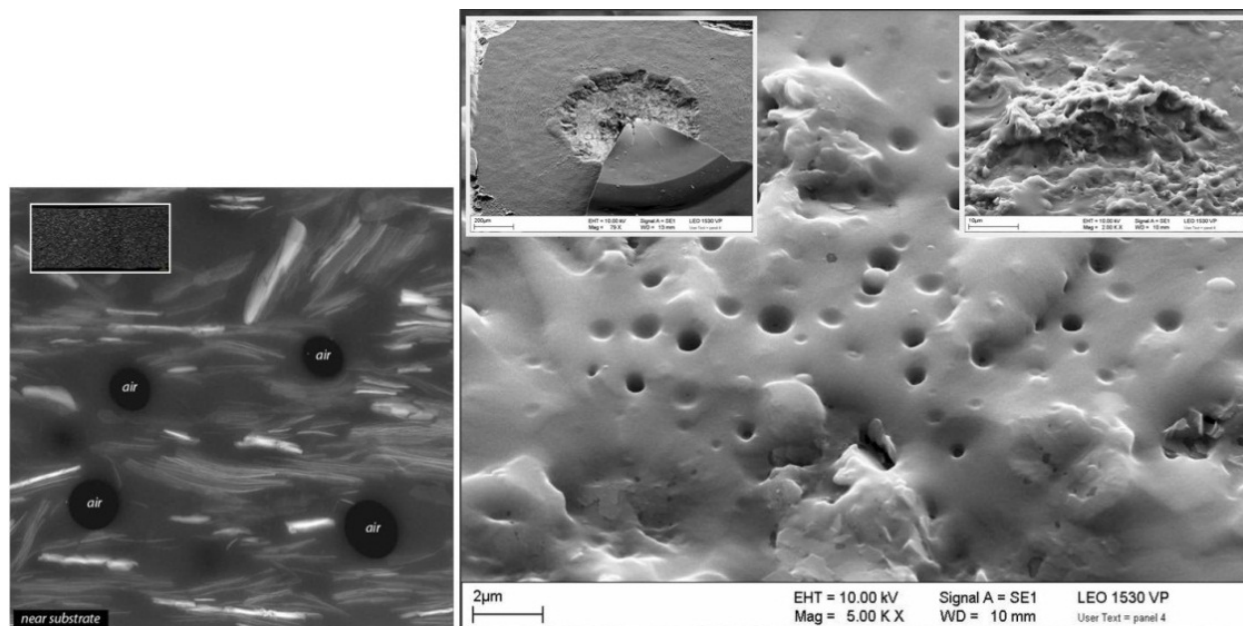


Figure 13. Impact crater from single spherical impact with increasing magnifications (inserts) showing spherical gaseous inclusions in the remnants of the primer layer obtained from the formulation also used to prepare the film shown in Fig. 12. (scale bar 2µm). A zoomed section of image Fig. 12 is shown for comparison. The term “air” is discussed in the text.

3.3. LDH based anti-corrosion coatings

As mentioned in section 2.5., the most effective corrosion inhibitor chromium ion Cr^{6+} used for years was banned from automotive coatings (Directive 2000/53/EC of the European Parliament and the council of 18 September 2000). In more details, it was declared in the European director that new vehicles after 1 July 2003 should not contain any lead, mercury, cadmium or hexavalent chromium, the latter being poisonous to the environment as well as being a potent carcinogen. Many chemical additives are also blacklisted by international regulations through REACH “Registration, Evaluation, Authorisation and Restriction of Chemicals” applied by the European Commission for enterprise and industry. With respect to metal substrates, such as aluminum and aluminum alloys like AA 2024-T3, commonly used in aeronautic, aerospace and automotive transportation, for the protective coatings these regulations apply. This prompted developments of chromate-free coatings anti-corrosion (Twite & Bierwagen, 1998; Sinko, 2001; Buchheit et al., 2003). To protect industrial ferrous and non-ferrous alloys as well as modern upcoming substrates from corrosion, applied coating technologies (spin coating, plasma, electrodeposition, anodization) and/or specific inhibitors (cerium, phosphate, molybdate, phosphate compounds, conducting polymers) may be selected (section 2.5.).

However the observation that a corrosion inhibitor dispersed into a coating may result in a weakening in its structure, leading to greater permeation trough diffusion mechanism and

finally to its deterioration led to the idea to prevent such deleterious phenomena by loading the inhibitor in some sort of “passive” container. Among possible containers LDH-type materials are of great interest due to their high lateral aspect ratio allowing efficient barrier properties as well as due to their ion exchange ability (see section 3.1.). The former arising from the strong structural platelets anisotropy is also to a great extent dependent on the degree of the particles dispersion within the coating. Once provided, reduction in gas (e.g. O_2) and electrolyte (e.g. H_2O and Cl^-) permeability through the polymer film should be expected through the creation of tortuous paths, thus decelerating the corrosion process (see section 2.4). With respect to the latter, the LDH host structure is acting as a scavenger towards aggressive ions (e.g. Cl^-), *vice et versa* Cl^- ions present a rather good affinity with LDH materials. Such ion entrapment is associated by displacing the interleaved anion, i.e. the corrosion inhibitor, if the ion exchange reaction proceeds. Reminding that LDH host structure is able to load very diverse anions, inhibition efficiency of intercalated inorganic or organic anions such as carbonate (Lin et al., 2007), molybdate (Yu et al., 2008), vanadate (Mahajanam & Buchheit, 2008; Zheludkevich et al., 2010) and laurate (Zhang et al., 2008a), quinaldate and thiazole derivative (Poznyak et al., 2009) has been reported recently.

Coating systems usually present pores and / or bear heterogeneities in the crosslink density from the sub-micrometer to the nano scale that facilitates the corrosion process to migrate along the metal coatings interface. Both cathodic and anodic corrosion mechanisms drastically increase or lower local pH values (see section 2.4.) respectively. Practically, an anodic corrosion process will induce a low pH value that would promote the dissolution of the LDH layer, thus buffering the medium as well as releasing the interleaved anion. On the contrary a cathodic corrosion process (i.e. oxygen evolution) imposes a high pH value that stabilizes the LDH phase that consequently would exchange either Cl^- or OH^- with the anti-corrosion agent. Hence such desorption triggered by the corrosion process may be viewed as a “smart” release of active molecules able to decrease the damaging on demand. It is also commonly designated as a “self-healing” behavior although the polymer phase is not repaired by the anticorrosion agent. In the anodic case, one should also mention that the dissolution of an appropriate LDH host framework could release Zn^{2+} ions into the media that are reported to act as an inhibitor to chloride-induced corrosion (Veleva et al., 1999; Williams & McMurray, 2003). In the following, one should distinguish between the barrier effect (passive inhibition) and the release of chemical agents (active inhibition). For the former, it is interesting to note that LDH-type barrier layers may be generated either chemically or electrochemically (section 3.1.). After prolonged immersion times in seawater, LDH-type material was found on the surface of composites and of monolithic 6092- and 6061-T6 aluminum panels (Ding et al., 2009). LDH / alumina bilayer film was fabricated on an Al foil via a single hydrothermal crystallization step (Guo et al., 2009) and topological growth of LDH platelets interleaved with surfactant molecules onto an aluminum substrate was reported to yield a super-hydrophobic protective film (Zhang et al., 2008). Due to the high cathodic corrosion activity of magnesium, a corrosion-resistant barrier forms on its surface in alkaline environments. In the presence of a trivalent metal in a basic medium, a LDH precursor is

deposited on the Mg alloy sheet (Buchheit & Martinez, 1998). Similarly, chemical conversion yielding a hydrotalcite (Mg,Al-LDH) was reported for a Mg-Al-Zn (AZ91D) alloy surface (Uan et al., 2008). No corrosion spot was observed after a 72 h salt spray test which was attributed to the formed protective barrier layer (Lin & Uan, 2009). Such a chemically-generation process may be further optimized using the separate nucleation and aging steps (SNAS) method which permits to form uniform and compact LDH films (Wang et al., 2010). Spin coating process was reported for AZ31 Mg alloy substrate (Zhang et al., 2008b), and spray-coated LDH formulation $\text{Mg}_3\text{Al}(\text{OH})_8\text{NO}_2 \cdot 2\text{H}_2\text{O}$ bearing nitrite ions onto a steel surface was claimed to result in a good corrosion resistance when immersed for 30-days into a 3% brine solution (Abe & Yasuda, 2005). Additionally to protect steel from corrosion during outdoor exposure over a long period of time, LDH barrier acts as a rust-inhibiting pigment when dispersed into an adhesion-promoting primer (Nagai et al., 2003; Sato et al., 2002) and such a “rustproofing” pretreatment of steel surfaces with a “paint-like” coating comprising a LDH formulation prior to painting was also reported (Yung et al., 2002; Sato et al., 2003) and related to overall coatings efficiency in the way that the procedure is enabling to reduce the number of coating stages (Nagai et al., 2004). For some coatings comprising zinc powder, formulations with hydrocalumite ($\text{Ca}_2\text{Al-LDH}$) as a fixing agent for corrosive ions provide a good adhesion to blast-treated steel plates as well as a high corrosion resistance in salt spray test (Kihira et al., 2007). Electrogenation of LDH particles reported for magnesium-based substrate was also found to improve the adhesion of subsequently applied paintings in addition to an enhanced corrosion resistance. Intercalated with corrosion inhibitor anions electrodeposited hydrotalcite films were claimed to adsorb corrosive ions and release corrosion inhibitor, and in the same time the LDH layer being firmly bound to the magnesium alloy (Yu et al., 2009). Similarly cathodic deposited coatings comprising LDH-like materials with an organic acid salt were claimed to provide excellent edge corrosion prevention, a high throwing power and chemical resistance along with other beneficial properties for film formation (Nakau et al., 2000).

For the release aspect, the beneficial effect to load the anti-corrosion agent into a LDH host structure is illustrated on Al 2024 as a substrate using nitrate $\text{Zn}_2\text{Al-LDH}$ ($\text{Zn}_2\text{Al}(\text{OH})_6(\text{NO}_3) \cdot 2\text{H}_2\text{O}$) that is a well-known model system for its anticorrosion efficiency (Miyata, 1988) (Fig. 14. & Fig. 15.). Figure 14 displays photographed specimens of epoxy based primer coated panels after an immersion test. The deleterious effect of the free nitrate is obvious if the extended corroded zones all over the exposed substrate area are compared to the much smaller domains that were formed when the equivalent amount of 2000 ppm nitrate had been embarked within the interstitial space of LDH platelets. This demonstrates the difference in (mobile) ionic strength throughout the test duration that facilitates diffusion of corrosive electrolyte in combination with a barrier effect imposed by the layered LDH particles. Additionally the beneficial effect of providing the inhibitor via an efficient triggered release from LDH hosts was observed on scratched and immersed panels which had been coated with the very same primer formulations and subsequently with a top coat (Fig. 15).

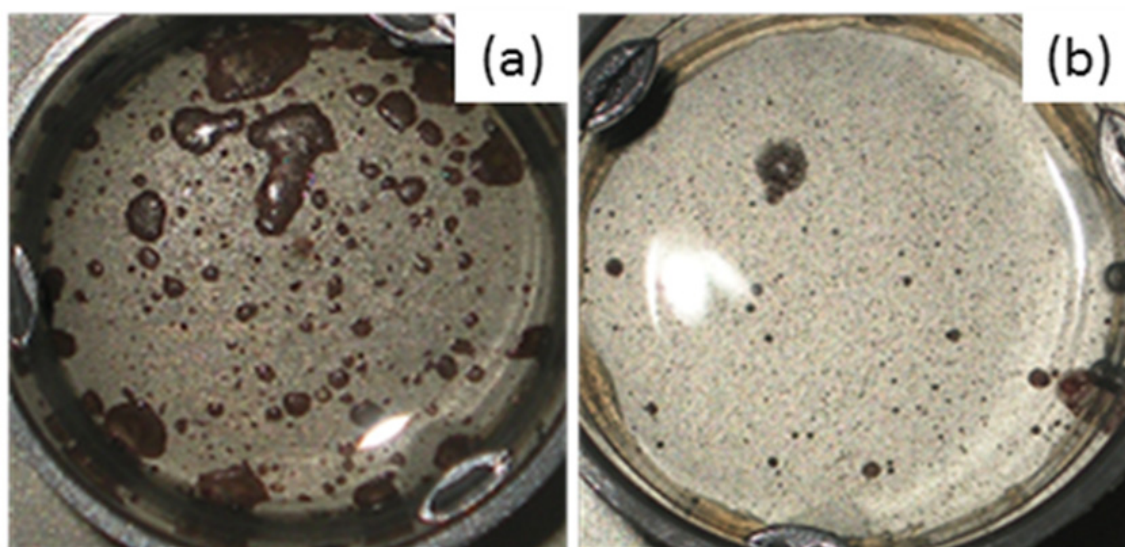


Figure 14. Epoxy primer coated panel, the primer comprising NaNO_3 (a) or LDH/ NO_3 (b) respectively. Panels were exposed to 0.005 M NaCl for 720 hours, the diameter of the exposed area being 4,6 cm. (Courtesy of Dr. Thomas Stimpfling)

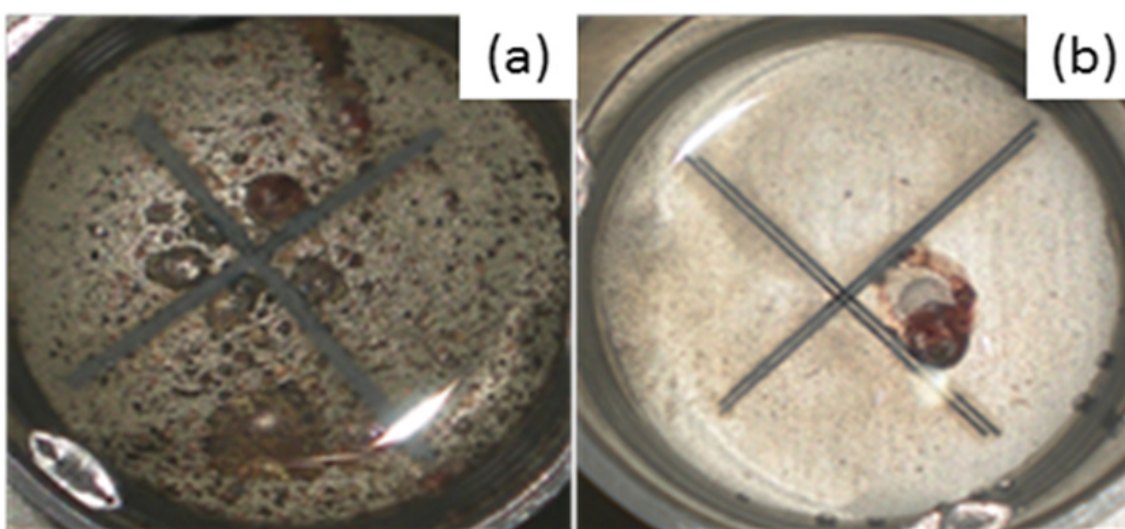


Figure 15. The same experimental set-up as described for figures 3a and 3b, except for an additional top coat being applied on the primer layer and that the coatings were scratched before exposure. (Courtesy of Dr. Thomas Stimpfling)

From pioneering work underlining the ability of LDH to act as a container for corrosion inhibiting species and in particular against filiform corrosion (Miyata, 1988), a lot of literature is now available. Most of them report the interest of LDH-based anti-corrosion coatings against blistering, pitting corrosion, visible and non-visible (sub layer electrolyte accumulation) damage zones involved in filiform corrosion and other corrosive reactions or coating failures. Similarly numerous patents report the relevance of LDH additives to prevent metal substrate corrosion; this is particularly well documented for Al-based alloys and steel substrates. Thus for coating AA2024-T3 alloy, a suitable composition was proposed that uses 2,5-dimercapto-1,3,4-thiadiazole (DMTD) as guest anion intercalated

between LDHs layers via the reconstruction method (Sinko & Kendig, 2005). DMTD does not form insoluble compounds with Al^{3+} but rather interacts locally at copper inclusions due to the high chemical affinity between the thiol and copper that results in a stable chemisorbed layer of the corresponding complexes. Deposited on the electrochemically active copper rich domains, it inhibits the oxygen reduction reaction. In succession LDH phases loaded with different thiazole derivatives like mercaptobenzothiazole, mercaptobenzimidazole, mercaptobenzotriazole, mercaptobenzoxazole, benzotriazole, or toloyltriazole were claimed to act in this vein (Price et al., 2010).

For steel-based substrates like low carbon steel plates vanadate bearing LDH hybrids as ion-exchangeable pigments in alkyd paints provide anticorrosive performance (Chico et al., 2008, however they were found to be less effective than zinc chromate. A special treatment providing a good corrosion resistance was reported for SPCC-SB (cold rolled carbon steel sheets or coils with dull or bright finish associated with standard temperature grade) sheets that is used for automotive modules, body panels and interior parts (Okumiya T, Ikematsu, 2007): LDH phases modified with saturated aliphatic monocarboxylic acids in admixture with magnesium acetate yield gels that can be applied on the rolled sheets in the form of the pulverized material. Finally synergistic corrosion inhibition for metal substrates in general and based on LDH was claimed (Gichuhi & Novelli, 2005): organic or inorganic corrosion inhibiting interleaved agents were selected according to the criteria of non-toxicity and to their ability to form stable, insoluble metal-ligand complexes, thus resulting in the protection of metal substrates and utilizing synergistic corrosion inhibitive mechanisms.

4. Conclusions

Within this chapter it was shown that modern and future automotive coatings might be realized which could either enhance resistance towards impact and corrosion to traditional systems or maintain their accustomed performance in more eco-efficient systems comprising less individual layers or in significantly thinner coatings by making use of layered particle based polymer composites. Following design principles for materials that combine tough failure with reinforcement and translating them into heterogeneous morphologies on varied length scales coatings damage due to stone impact can effectively be limited. By tuning the compatibility between the components of the polymer matrix as well as the affinity between these and layered inorganic particles of a toolbox of some polyesters, polyurethanes and layered double hydroxides such different coatings morphologies like disperse, bi-continuous, stratified as well as textured structures can be obtained, all of them performing outstandingly as a primer layer of an automotive coating system in stone impact tests.

Contrary to some other layered inorganic particles like Montmorillonite as well as compared to other encapsulation materials like polyelectrolytes or hard polymer capsules it is the chemical and structural variability in combination with both their chemical stability under moderate conditions and their structural lability in more acidic as well as basic environments that renders layered double hydroxides versatile host materials for corrosion inhibiting species. Such hybrid particles thus act on different time scales and in different modes in a polymer matrix which yields at low loadings multifunctional organic coatings:

1. Mechanical reinforcement and stress dissipation.
2. Diffusion barrier towards oxygen and humidity.
3. Triggered release of corrosion inhibitors.
4. Buffering local changes in pH value via structural decomposition.
5. Supply of chemical components for the formation of passivation layers and in the case of deposited LDH-like phases an adhesion promoting layer might be of relevance for repair coatings thus acting similar to a conversion layer.

The latter aspect deserves further investigations with respect to zinc, aluminium and magnesium based alloys that are progressively used as materials in especially light weight automotive body construction. Recent investigations of corrosion processes have shown that layered double hydroxides are deposited as passivating surface layers in the course of the anodic reaction.

Additionally related to high aspect ratios and the ability to assemble into ordered lyotropic mesophases layered double hydroxide particles based formulations could yield textured films that are attractive regarding automotive effect coatings which demand highly oriented layered effect pigments like aluminium flakes or mica platelets in order to provide highest possible viewing angle dependent optical properties of the coating. Thus it was recently proposed that the LDH based aqueous formulation that has been described in the context of impact resistance in this chapter might be used to impose its tendency to form ordered films on the pigment orientation parallel to the substrates surface (Hintze-Bruening et al., 2010).

Author details

Horst Hintze-Bruening
BASF Coatings GmbH, Germany

Fabrice Leroux
Clermont University, CNRS, France

5. References

- Abe, Y & Yasuda, M. (2005). Hydrotalcite-containing inorganic coatings showing long-lasting anticorrosive property, JP2005112998.
- Alemдар, A. & Buetuen, V. (2005). Interaction between a Tertiary Amine Methacrylate Based Polyelectrolyte and a Sodium Montmorillonite Dispersion and Its Rheological and Colloidal Properties. *Journal of Applied Polymer Science*, Vol.95,pp. 300–306.
- Alvarez, D.; Collazo, A.; Hernandez, M.; Novoa, XR. & Perez, C. (2010). Corrosion protective properties of hydrotalcites doped hybrid sol-gel coatings on aluminium substrates, *Materials Science Forum*, Vol. 636-637, pp. 996-1003.
- Balazs, A.C.; Singh, C. & Zhulina, E. (1998). Modeling the Interactions between Polymers and Clay Surfaces through Self-Consistent Field Theory. *Macromolecules*, Vol. 31, pp. 8370-8381.

- Bender, H. (1969). The mechanical properties of films and their relation to paint chipping. *Journal of Applied Polymer Science*, Vol. 13, pp. 1253-1264.
- Bonderer, L.J.; Studart, A.R. & Gauckler, L.J. (2008). Bioinspired Design and Assembly of Platelet Reinforced Polymer Films. *Science*, Vol. 319, pp. 1069-1073.
- Bookin, S.; Cherkashin, V.I. & Drits, V.A. (1993). Polytype diversity of the hydrotalcite-like minerals. II. Determination of the polytypes of experimentally studied varieties. *Clays and Clay Minerals*, Vol.41, pp. 558-564.
- Buchheit, RG.; Guan, H.; Mahajanam, S. & Wong, F. (2003). Active corrosion protection and corrosion sensing in chromate-free organic coatings. *Progress in Organic Coatings*, vol.47, pp. 174-182.
- Buchheit, RG. & Martinez, MA. (1998). Formation of corrosion-resistant oxide coating on metal or alloy surface in alkaline bath, US985756218.
- Cauvin, S.; Colver, P.J. & Bon, S.A.F. (2005). Pickering Stabilized Miniemulsion Polymerization: Preparation of Clay Armored Latexes. *Macromolecules*, Vol. 38, pp. 7887-7889
- Chen, H.; Zhang, F.; Fu, S. & Duan, X. (2006). In situ microstructure control of oriented layered double hydroxide monolayer films with curved hexagonal crystals as superhydrophobic materials. *Advanced Materials*, Vol.18, pp. 3089-3093.
- Chico, B.; Simancas, J. ; Vega, JM.; Granio, N.; Diaz, I.; de la Fuente, D. & Morcillo, M. (2008). Anticorrosive behavior of alkyd paints formulated with ion-exchange pigments. *Progress in Organic Coatings*, Vol.61, pp. 283-290.
- Cousin, F.; Cabuil, V. & Levitz, P. (2002). Magnetic Colloidal Particles as Probes for the Determination of the Structure of Laponite Suspensions. *Langmuir*, Vol. 18, pp. 1466-1473.
- Dhar, S.; Krajac, T.; Ciampini, D. & Papini, M. (2005). Erosion mechanisms due to impact of single angular particles. *Wear*, Vol. 258, pp. 567-579.
- Di, J. & Sogah, D.Y. (2006). Exfoliated Block Copolymer/Silicate Nanocomposites by One-Pot, One-Step in-Situ Living Polymerization from Silicate-Anchored Multifunctional Initiator. *Macromolecules*, Vol. 39, pp. 5052-5057.
- Dijkstra, M.; Hansen, J.-P. & Madden, P.A. (1997). Statistical model for the structure and gelation of smectite clay suspensions. *Physical Review E*, Vol. 55, pp. 3044-3053.
- Ding, H.; Hawthorn, GA. & Hihara, LH. (2009). Inhibitive effect of seawater on the corrosion of particulate-reinforced aluminum-matrix composites and monolithic aluminum alloy. *Journal of Electrochemical Society*, Vol.156, pp. C352-C359.
- Dioh, N.N. & Williams J.G. (1994). The impact behavior of paints. *Journal of Materials Science*, Vol. 29, pp. 6091-6096.
- Fukushima, Y.; Okada, A.; Kawasumi, M; Kurauchi, T. & Kamigaito, O. (1988). Swelling behavior of Montmorillonite by Poly-6-amide. *Clay Minerals*, Vol. 23, pp. 27-34.
- Gao, H.; Ji, B.; Jaeger, I.L.; Arzt, E. & Fratzl, P. (2003). Materials become insensitive to flaws at nanoscale: Lessons from nature. *Proceedings of the National Academic Society*, Vol. 100, pp. 5597-5600.
- Gao, YF.; Nagai, M.; Masuda, Y.; Sato, F.; Seo WS. & Koumoto, K. (2006). Surface precipitation of highly porous hydrotalcite-like film on Al from a zinc aqueous solution. *Langmuir*, Vol.22, pp. 3521-3527.

- Garcés, J.M.; Moll, D.J.; Bicerano, J.; Fibiger, R. & McLeod, D.G. (2000). Polymeric Nanocomposites for Automotive Applications. *Advanced Materials*, Vol. 12, pp. 1835-1839.
- Gatos, K.G. & Karger-Kocsis, J. (2007). Effect of the aspect ratio of silicate platelets on the mechanical and barrier properties of hydrogenated acrylonitrile butadiene rubber (HNBR)/layered silicate nanocomposites. *European Polymer Journal*, Vol. 43, pp. 1097-1104.
- Géraud, E.; Prevot, V.; Ghanbaja J. & Leroux, F. (2006). Macroscopically ordered hydrotalcite-type materials using self-assembled colloidal crystal template. *Chemistry of Materials*, Vol.18, pp. 238-240.
- Gersappe, D. (2002). Molecular Mechanisms of Failure in Polymer Nanocomposites. *Physical Review Letters*, Vol. 89, pp. 058301-1 – 058301-4.
- Gichuhi, T. & Novelli W. (2005). Synergistic corrosion inhibitor for metal substrates based on hydrotalcite or layered double hydroxide complexing agents, US20050235873.
- Ginzburg, V.V.; Qiu, F.; Paniconi, M.; Peng, G.; Jasnow, D. & Balazs, A.C. (1999). Kinetic model of phase separation in binary mixtures with hard mobile impurities. *Physical Review E*, Vol. 60, pp. 4352-4359.
- Ginzburg, V.V.; Qiu, F.; Paniconi, M.; Peng, G.; Jasnow, D. & Balazs, A.C. (1999). Simualtion of hard particles in a phase-separating binary mixture. *Physical Review Letters*, Vol. 82, pp. 4026-4029.
- Gosh, B. & Urban, M. (2009). Self-repairing oxetane substituted chitosan polyurethane networks. *Scienc*, Vol.323, pp. 1458-1460
- Guo, X. ; Xu, S. ; Zhao, L. ; Lu, W. ; Zhang, F. ; Evans, DG. & Duan, X. (2009). One-Step Hydrothermal Crystallization of a Layered Double Hydroxide/Alumina Bilayer Film on Aluminum and Its Corrosion Resistance Properties. *Langmuir*, Vol. 25, pp. 9894-9897.
- Gupta, V.; Gupta, S. & Miura, N. (2008). Potentiostatically deposited nanostructured $\text{Co}_x\text{Ni}_{1-x}$ layered double hydroxides as electrode materials for redox-supercapacitors. *Journal of Power Sources*, Vol. 175, pp. 680-685.
- Gurski, JA.; Blough, SD.; Luna, C.; Gomez, C.; Luevano A.N. & Gardner, EA. (2006). Particle-particle interactions between layered double hydroxide nanoparticles. *Journal of American Chemical Society*, Vol. 128, pp. 8376-8377.
- Hibino T. & Kobayashi, M. (2005). Delamination of layered double hydroxides in water. *Journal of Materials Chemistry*, Vol.15, pp. 653-656.
- Hintze-Bruening, H. ; Troutier-Thuilliez, A.-L. & Leroux, F. (2009). Layered particle-based polymer composites for coatings: Part II—Stone chip resistant automotive coatings. *Progress in Organic Coatings*, Vol. 64, pp. 193-204.
- Hintze-Bruening, H. ; Steiner, H.-P.; Leroux, F.; Troutier-Thuilliez, A.-L. & Stimpfling, T. (2010). WO2010130308.
- Hintze-Bruening, H. ; Troutier-Thuilliez, A.-L. & Leroux, F. (2011). Layered particle-based polymer composites for coatings: Part III— Textured coatings obtained via lyotropic liquid Crystals. *Progress in Organic Coatings*, Vol. 70, pp. 240-244.
- Hintze-Bruening, H.; Dornbusch, M.; Toews, S. & Bremser, W. (2011). Method for autophoretic coating, coating agent and multilayer paint finish. WO2011138290.
- Hu G. & O'Hare, D. (2005). Unique layered double hydroxide morphologies using reverse microemulsion synthesis. *Journal of American Chemical Society*, Vol.127, pp. 17808-17813.

- Huang, X. & Brittain, W.J. (2001). Synthesis and Characterization of PMMA Nanocomposites by Suspension and Emulsion Polymerization. *Macromolecules*, Vol. 34, pp. 3255-3260.
- Hughes, A.E.; Cole, I.S.; Muster, T.H. & Varley, R.J. (2010). Designing green, self-healing coatings for metal protection. *NPG Asia Materials*, Vol.2, pp. 143-151.
- Indira, L. & Kamath, P.V. (1994). Electrogenation of base by cathodic reduction of anions: novel one-step route to unary and layered double hydroxides (LDHs). *Journal of Materials Chemistry*, Vol.4, pp. 1487-1490.
- Ji, Y.-Q.; Black, L.; Weidler, P.G. & Janek, M. (2004). Preparation of Nanostructured Materials by Heterocoagulations Interaction of Montmorillonite with Synthetic Hematite Particles. *Langmuir*, Vol. 20, pp. 9796-9806.
- Joensson, B.; Labbez, C. & Cabane, B. (2008). Interaction of Nanometric Clay Platelets. *Langmuir*, Vol. 24, pp. 11406-11413.
- Jung, C. ; Schimakura, T. ; Maurus, N. & Domes, H. (2002). Method for pretreating and/or coating metallic surfaces with a paint-like coating prior to forming and use of substrates coated in this way, WO02031064.
- Kanai, T. & Nomura H. (2009). Metals surface-treated with crosslinked polysiloxanes, their manufacture, and surface treating liquids containing alkoxysilanes or their hydrolyzates, JP2009262402.
- Karim, A.; Douglas, J.F.; Nisato, G.; Liu, D.-W. & Amis, E.J. (1999). Transient Target Patterns in Phase Separating Filled Polymer Blends. *Macromolecules*, Vol. 32, pp. 5917-5924.
- Kihira, H.; Aiga, T.; Imai, A.; Hiramatsu, K.; Mitsutsuka, Y.; Nagai, M.; Sato, T. & Matsumoto, T. (2007). Anticorrosive zinc dust-containing coating compositions, JP2007284600.
- Kreis, W.; 26th European Car Body Conference, Bad Nauheim, 27 Febr. 2008
- Kugge, C.; Vanderhoek, N. & Bousfield, D.W. (2011). Oscillatory shear response of moisture barrier coatings containing clay of different shape factor. *Journal of Colloid and Interface Science*, Vol. 358, pp. 25-31.
- Lagaly, G.; Stange, H. & Weiss, A. (1973). Adsorption of long chain molecules onto aromatic swelling liquids in mica type layer silicate. *Proceedings of the International Clay Conference, Madrid*, pp. 693-704.
- Lagaly, G.; Beneke, K. & Weiss, A. (1975). Magadiite and H-Magadiite: II. H-Magadiite and its intercalation compounds. *American Mineralogist*, Vol.60, pp. 650-658
- Lagaly, G. (1981). Characterization of clays by organic compounds. *Clay Minerals*, Vol. 16, pp. 1-21.
- Lan, T.; Kaviratna, P.D. & Pinnavaia, T.J. (1996). Epoxy self-polymerization in smectite clays. *Journal of Physics and Chemistry of solids*, Vol.57, pp. 1005-1010.
- Lepoittevin, B.; Pantoustier, N.; Devalckenaere, M.; Alexandre, M.; Kubies, D.; Calberg, C. ; Jérôme, R. & Dubois, P. (2002). Poly(e-caprolactone)/Clay Nanocomposites by in-Situ Intercalative Polymerization Catalyzed by Dibutyltin Dimethoxide. *Macromolecules*, Vol. 35, pp. 8385-8390.
- Leroux, F.; Stimpfling, T. & Hintze-Bruening, H. (2012). Relevance and Performance of LDH Platelets in Coatings. *Recent Patents on Nanotechnology*, Vol. 6, accepted

- Lin, J. K.; Hsia, C. L. & Uan, J. Y. (2007). Characterization of Mg,Al-hydrotalcite conversion film on Mg alloy and Cl⁻ and anion-exchangeability of the film in a corrosive environment. *Scripta Materialia*, Vol.56, pp. 927-930.
- Lin, J.K. & Uan, J.Y. (2009). Formation of Mg,Al-hydrotalcite conversion coating on Mg alloy in aqueous HCO₃⁻/CO₃²⁻ and corresponding protection against corrosion by the coating. *Corrosion Science*, vol.51, pp. 1181-1188.
- Liu, Z.; Ma, R.; Osada, M.; Iyi, N.; Ebina, Y.; Takada, K. & Sasaki, T. (2006). Synthesis, anion exchange, and delamination of Co-Al layered double hydroxide: assembly of the exfoliated nanosheet/polyanion composite films and magneto-optical studies. *Journal of American Chemical Society*, Vol.128, pp. 4872-4880.
- Lonyuk, M.; Bosmab, M.; Riemsdag, A.C.; Zuidema, J.; Bakker, A. & Janssen, M. (2007). Stone-impact damage of automotive coatings: A laboratory single-impact tester. *Progress in Organic Coatings*, Vol.58, pp. 241-247.
- Lonyuk, M.; Bosmab, M.; Vijverberg, C.A.M.; Bakker, A. & Janssen, M. (2008). Relation between chip resistance and mechanical properties of automotive coatings. *Progress in Organic Coatings*, Vol.61, pp. 308-315.
- Luan, L.; Li, W.; Liu, S. & Sun, D. (2009). Phase behavior of mixtures of positively charged colloidal platelets and nonadsorbing polymer. *Langmuir*, Vol. 25, pp. 6349-6356.
- Mahajanam, S. P. V. & Buchheit, R. G. (2008). Characterization of Inhibitor Release from Zn-Al-[V₁₀O₂₈]⁶⁻ Hydrotalcite Pigments and Corrosion Protection from Hydrotalcite-Pigmented Epoxy Coatings. *Corrosion*, Vol.64, pp. 230-240.
- Makowski, M.P.; Martz, J.T.; Novak, C.A. & Verardi, C.A. (2005). Coatings with improved chip resistance and methods of making the same. WO2005052077.
- Milczewska, K.; Voekel, A. & Jeczalik, J. (2003). The use of Flory-Huggins parameter to characterization of polymer/filler interaction. *Macromolecular Symposia*, Vol. 194, pp. 305-311.
- Miyata S. (1988). Filiform corrosion-resistant primer coating composition and preventing filiform corrosion with hydrotalcite inhibitors. US884761188.
- Mourad, M.C.D. Devid, E.J.; van Schooneveld, M.M.; Vonk, C. & Lekkerkerker, H.N.W. (2008). Formation of nematic liquid crystals of sterically stabilized layered double hydroxide platelets. *Journal of Physical Chemistry B*, Vol.112, pp. 10142-10152.
- Mourchid, A.; Delville, A.; Lambard, J.; LeColier, E. & Levitz, P. (1995). Phase Diagram of Colloidal Dispersions of Anisotropic Charged Particles: Equilibrium Properties, Structure, and Rheology of Laponite Suspensions. *Langmuir*, Vol. 11, pp. 1942-1950.
- Nagai, M.; Sato, T.; Taki, T.; Yamazaki, A. & Tanabe H. (2003). Corrosion protection of weather-resistant steels with moisture-curable primers. JP2003082477.
- Nagai, M.; Taki, T.; Sato, T.; Matsuno, H. & Yamazaki, A. (2004). Corrosion prevention of weather- and rust-resistant steels with less number of coating stages. JP2004097945.
- Nakao, F.; Sugisaki, K. & Tominaga, A. (2000). Cationically electrodepositable coating material. EP001046684.
- Ogawa M. & Kaiho, H. (2002). Homogeneous precipitation of uniform hydrotalcite particles. *Langmuir*, Vol.18, pp. 4240-4242.

- Okamoto, K.; Sasaki, T.; Fujita, T. & Iyi, N. (2006). Preparation of highly oriented organic-LDH hybrid films by combining the decarbonation, anion-exchange, and delamination processes. *Journal of Materials Chemistry*, Vol.16, pp. 1608-1616.
- Okumiya, T. & Ikematsu, D. (2007). Aqueous anticorrosive coatings containing layered double hydroxides exfoliated in water and metalis substrates coated therewith. JP2007039549.
- Pang, J.W.C. & Bond, I.P. (2005). 'Bleeding composites' – damage detection and self-repair using a biomimetic approach. *Composites: Part A*, Vol. 36, pp. 183-188
- Paulhiac, J.L. & Clause, O. (1993). Surface coprecipitation of cobalt(II), nickel(II), or zinc(II) with aluminium(III) ions during impregnation of γ -alumina at neutral pH. *Journal of American Chemical Society*, Vol.115, pp. 11602-11603.
- Pignon, F.; Magnin, A.; Piau, J.-M.; Cabane, B.; Lindner, P. & Diat, O. (1997). Yield stress thixotropic clay suspension: investigations of structure by light, neutron and X-ray scattering. *Physical Review E*, Vol. 56, pp. 3281-3289.
- Poznyak, S. K.; Tedim, J.; Rodrigues, L. M.; Salak, A. N.; Zheludkevich, M. L.; Dick, L. F. P. & Ferreira, M. G. S. (2009). Novel Inorganic Host Layered Double Hydroxides Intercalated with Guest Organic Inhibitors for Anticorrosion Applications. *ACS Applied Materials & Interfaces* Vol.1, pp. 2353-2362.
- Prevot, V.; Forano, F. & Besse, J.P. (2005). Hydrolysis in polyol: new route for hybrid-layered double hydroxides preparation. *Chemistry of Materials*, Vol.17, pp. 6695-6701.
- Price, C.; Matzdorf, C.; Nickerson, W. & Lipnickas, E. (2010). Magnesium-rich anticorrosive coating compositions. US20100197836.
- Ramamurthy, A.C.; Lorenzen, W.I. & Bless, S.J. (1994). Stone impact damages to automotive paint finishes: an introduction to impact physics and impact induced corrosion. *Progress in Organic Coatings*, Vol.25, pp. 43-71.
- Rao, Y.Q. & Pochan, J.M. (2007). Mechanics of Polymer-Clay Nanocomposites. *Macromolecules*, Vol. 40, pp. 290-296.
- Ritchie, R.O. (2011). The conflicts between strength and toughness. *Nature Materials*, Vol. 10, pp. 817-822.
- Roesler, M.; Klinke, E. & Kunz, G. (1997). Glashohlkugeln als stossabsorbierende Fuellstoffe. *Farbe und Lack*, Vol.103, pp. 49-54.
- Rutherford, K.L.; Trezona, R.I.; Ramamurthy, A.C. & Hutchings, I.M. (1997). The abrasive and erosive wear of polymeric paint films. *Wear*, Vol. 203-204, pp. 325-334.
- Ryntz, R.A.; Ramamurthy, A.C. & Holubka, J.W. (1995). Stone impact damage to painted plastic substrates. *Journal of Coatings Technology*, Vol. 67, pp. 23-31.
- Ryntz, R.A.; Ramamurthy, A.C. & Mihora, D.J. (1995). Thermal and impact induced stress failure in painted TPO: the role of surface morphology. *Journal of Coatings Technology*, Vol. 67, pp. 35-46.
- Sato, T.; Nomura, R.; Maekawa, S. & Yamazaki, A. (2002). Agent for steel surface preparation prior to painting. JP2002285362.
- Sato, T.; Yamazaki, A. & Matsuno, H. (2003). Surface conditioning agents of steel for paint coating. JP2003328162.
- Shah, D.; Maiti, P.; Gunn, E.; Schmidt, D.F.; Jiang, D.D.; Batt, C.A. & Giannelis, P. (2004). Dramatic enhancements in toughness of polyvinylidene fluoride nanocomposites via

- nano-clay directed crystal structure and morphology. *Advanced Materials*, Vol. 16, pp. 1173-1177.
- Shah, D.; Maiti, P.; Jiang, D.D.; Batt, C.A. & Giannelis, P. (2005). Effect of nanoparticle mobility on toughness of polymer nanocomposites. *Advanced Materials*, Vol. 17, pp. 525-528.
- Shalkevich, A.; Stradner, A.; Bhat, S.K.; Muller, F. & Schurtenberger, P. (2007). Cluster, Glass, and Gel Formation and Viscoelastic Phase Separation in Aqueous Clay Suspensions. *Langmuir*, Vol. 23, pp. 3570-3580.
- Sinko, J. (2001). Challenges of chromate inhibitor pigments replacement in organic coatings. *Progress in Organic Coatings*, Vol.42, pp. 267-282.
- Sinko, J. & Kendig, MW. (2005). Pigment-grade corrosion inhibitors for protective coating on metal substrates. WO2005003408.
- Studart, A.R.; Gonzenbach, U.T.; Tervoort, E. & Gauckler, L.J. (2006). Processing Routes to Macroporous Ceramics: A Review. *Journal of the American Ceramic Society*, Vol.89, pp. 1771-1789.
- Toohey, K.S.; Sottos, N.R. & White, S.R. (2009). Characterization of Microvascular-Based Self-healing Coatings. *Experimental Mechanics*, Vol.49, pp. 707-717
- Triantafyllidis, K.S.; LeBaron, P.C.; Park, I. & Pinnavaia, T.J. (2006). Epoxy-Clay Fabric Film Composites with Unprecedented Oxygen-Barrier Properties. *Chemistry of Materials*, Vol. 18, pp. 4393-4398.
- Troutier-Thuilliez, A.-L. ; Taviot-Guéhoa, C. ; Cellier, J. ; Hintze-Bruening, H. & Leroux, F. (2009). Layered particle-based polymer composites for coatings: Part I. Evaluation of layered double hydroxides. *Progress in Organic Coatings*, Vol. 64, pp. 182-192.
- Troutier-Thuilliez, A.-L.; Hintze-Bruening, H.; Taviot-Guého, C.; Verney, V. & Leroux, F. (2011). Exfoliation and liquid crystal phase formation of layered double hydroxide into waterborne polyurethane coatings. *Soft Matter*, Vol.7, pp. 4242-4251.
- Twite, RL. & Bierwagen, GP. (1998). Review of alternatives to chromate for corrosion protection of aluminium aerospace alloys. *Progress in Organic Coatings*, Vol.33, pp. 91-100.
- Uan, J-Y.; Yu, B-L. & Pan X-L. (2008). Morphological and microstructural characterization of the aragonitic $\text{CaCO}_3/\text{Mg,Al}$ -hydrotalcite coating on Mg - 9 Wt Pct Al - 1 Wt Pct Zn alloy to protect against corrosion. *Metal Materials Transaction A*, Vol.39, pp. 3233-3245.
- Veleva, L.; Chin, J. & del Amo, B. (1999). Corrosion electrochemical behavior of epoxy anticorrosive paints based on zinc molybdenum phosphate and zinc oxide. *Progress in Organic Coatings*, Vol.36, pp. 211-216.
- Volovitch, P.; Vu, T.N.; Allély, C. ; Aal, A.A. & Ogle K. (2011). Understanding corrosion via corrosion product characterization: II. Role of alloying elements in improving the corrosion resistance of Zn-Al-Mg coatings on steel. *Corrosion Science*, Vol.53, pp. 2437-2445
- Wang, JA.; Morales, A.; Bokhimi, X.; Novaro, O.; Lopez, T. & Gomez, R. (1999). Cationic an anionic vacancies in the crystalline phases of sol-gel magnesia-alumina catalysts. *Chemistry of Materials*, Vol.11, pp. 308-313.
- Wang, J. ; Li, D. ; Yu, X.; Jing, X.; Zhang, M. & Jiang, Z. (2010). Hydrotalcite conversion coating on Mg alloy and its corrosion resistance. *Journal of Alloys Compounds*, Vol. 494, pp. 271-274.

- Wang, X.; Gao, Y.; Mao, K.; Xue, G.; Chen, T.; Zhu, J.; Li, B.; Sun, P.; Jin, Q. & Ding, D. (2006). Unusual Rheological Behavior of Liquid Polybutadiene Rubber/Clay Nanocomposite Gels: The Role of Polymer-Clay Interaction, Clay Exfoliation, and Clay Orientation and Disorientation. *Macromolecules*, Vol. 39, pp. 6653-6660.
- Weber, B.; Bremser, W. & Hiltrop, K. (2009). Creating new materials with melamine resins. *Progress in Organic Coatings*, Vol.64, pp. 150-155.
- Williams, G. & McMurray, H. N. (2003). The mechanism of group (I) chloride initiated filiform corrosion on iron. *Electrochemistry Communications*, Vol.5, pp. 871-877.
- Xu, ZP.; Stevenson, G.; Lu, CQ.; Lu, GQ.; Bartlett, P. & Gray, P. (2006). Stable suspension of layered double hydroxide nanoparticles in aqueous solution. *Journal of American Chemical Society*, Vol.128, pp. 36-37.
- Yu, X.; Wang, J.; Zhang, M.; Yang, L.; Li, J.; Yang, P. & Cao, D. (2008). Synthesis, characterization and anticorrosion performance of molybdate pillared hydrotalcite/in situ created ZnO composite as pigment for Mg-Li alloy protection. *Surface and Coatings Technology*, Vol.203, pp. 250-255.
- Yu, X.; Li, J.; Wang, J.; Jing, X. & Zhang, M. (2009). Electrodeposition method for forming corrosion inhibitor anion-intercalated hydrotalcite film on magnesium alloy surface. CN200910072431.
- Yurekli, K.; Karim, A.; Amis, E.J. & Krishnamoorti, R. (2003). Influence of Layered Silicates on the Phase-Separated Morphology of PS-PVME Blends. *Macromolecules*, Vol. 36, pp. 7256-7267.
- Yurekli, K.; Karim, A.; Amis, E.J. & Krishnamoorti, R. (2004). Phase Behavior of PS-PVME Nanocomposites. *Macromolecules*, Vol. 37, pp. 507-515.
- Zang, J.; Luan, L.; Zhu, W.; Liu, S. & Sun, D. (2007). Phase behavior of aqueous suspensions of Mg₂Al layered double hydroxide: the competition among nematic ordering, sedimentation, and gelation. *Langmuir*, Vol.23, pp. 5331-5337.
- Zehnder, A.T.; Ramamurthy, A.C.; Bless, S.J. & Brar, N.S. (1993). Stone impact damages to automotive paint finishes: measurement of temperature rise due to impact. *International Journal of Impact Engineering*, Vol.13, pp. 133-143.
- Zhang, F.; Zhao, L.; Chen, H.; Xu, S.; Evans, D. G. & Duan, X. (2008a). Corrosion Resistance of Superhydrophobic Layered Double Hydroxide Films on Aluminum. *Angewandte Chemie International Edition*, Vol.47, pp. 2466-2469.
- Zhang, F.; Sun, M.; Xu, S.; Zhao, L. & Zhang, B. (2008b). Fabrication of oriented layered double hydroxide films by spin coating and their use in corrosion protection. *Chemical Engineering Journal*, Vol.141, pp. 362-367.
- Zhao, Y.; Li, F.; Zhang, R.; Evans, DF. & Duan, X. (2002). Preparation of layered double-hydroxide nanomaterials with a uniform crystallite size using a new method involving separate nucleation and aging steps. *Chemistry of Materials*, Vol.14, pp. 4286-4291.
- Zheludkevich, M. L.; Poznyak, S. K.; Rodrigues, L. M.; Raps, D.; Hack, T.; Dick, L. F.; Nunes, T. & Ferreira, M. G. S. (2010). Active protection coatings with layered double hydroxide nanocontainers of corrosion inhibitor. *Corrosion Science*, Vol.52, pp. 602-611.
- Zouari, B. & Touratier, M. (2002). Simulation of organic coating removal by particle impact. *Wear*, Vol. 253, pp. 488-497.